

Polymer Free Volume and Its Connection to the Glass Transition

RONALD P. WHITE and JANE E.G. LIPSON*

Department of Chemistry,
Dartmouth College, Hanover, NH 03755

Abstract

In this Perspective we summarize the most widely-used definitions of free volume and illustrate the differences between them, including the important distinction between *total* free volume and *excess* free volume. We discuss the implications when alternative estimates for free volume are inserted into relationships that connect experimentally-measured properties (e.g. the viscosity) to free volume, such as those proposed by Doolittle, Fox and Flory, Simha and Boyer, Cohen and Turnbull, and Williams, Landel, and Ferry. Turning to the results of our own Locally Correlated Lattice (LCL) model we demonstrate, by analyzing data for a set of over fifty polymers, that our calculations for total percent free volume not only lead to a predictive relationship with experimental glass transition temperatures, but also allow us to place the different definitions of free volume within a physical picture of what the proposed contributions represent. We find that melts go glassy upon reaching a 'boundary' of minimum (total) percent free volume that depends roughly linearly on temperature. We interpret this boundary as being close to the T -dependent free volume associated with solid-like segmental vibrational motions. Since the LCL model is a first principles thermodynamic theory we are also able to link our free volume predictions to similar patterns that we find in the predicted entropy per theoretical segment. Our results are consistent with a picture wherein the difference in entropy between the melt (liquid) state and corresponding solid state vanishes as the glass transition is approached. This leads us to a new connection with the work of Adams and Gibbs, whose model reflects a similar vanishing of the configurational entropy. We conclude by discussing why the approach to the glassy state is best viewed as being controlled via the *linked* contributions of free volume and temperature.

I. Introduction

The notion that "free volume" can be used to explain some aspect of polymeric behavior or properties is controversial.¹⁻⁹ Since the fraction of unoccupied volume in a melt or glassy sample cannot be directly measured, then estimates of fractional free volume are tied to the particular choice of model. The result is that the term has more than one meaning, and every estimate *should* be tethered to how it has been obtained. The italics highlight a significant issue, one that plagues other 'characteristic' quantities in polymer science, e.g. the so-called chi parameter, and the solubility parameter. However, the lack of clarity in discussions regarding free volume have resulted in significant resistance to its possible utility.

In this work we begin with a summary of how the concept of polymeric free volume was introduced and then propagated. Going further, we provide a physical picture of these various measures of free volume, as well as our own. With respect to the latter, we describe a clear and unambiguous route for calculating the theoretical percent free volume, using the Locally Correlated Lattice (LCL) model,^{10,11} and show that its temperature dependence leads to a surprisingly good prediction of the glass transition temperature (T_g). Some preliminary results were presented in ref 10; here we delve much further. From tracking the free volumes of 51 polymer melts down to their respective experimental T_g values, we obtained a T -dependent trend that we interpret as the minimum free volume that a polymer must have to still be in the melt state. Or, viewed another way, it represents an upper bound for percent free volume that can still be accommodated by a glass. This boundary line lies a few percent above the (T -dependent) contributions associated with solid-like (segmental vibrational) behavior. Our picture of what happens to the excess (liquid minus solid-like) free volume as a melt cools, is reminiscent of what is anticipated to happen to the excess entropy as it decreases on its way toward the ideal glass transition. In fact, we also show that there is a close relationship between the percent free volume and the LCL entropy per theoretical segment, which allows us to draw connections with the theory of Adam and Gibbs.¹² The end

result is a new contribution to understanding how free volume, entropy, and temperature, play their respective roles in the glassification of melts.

Some decades ago the concept of free volume became popularized as a means to explain and quantify the changes in dynamic and mechanical properties e.g., viscosity (η), relaxation times (τ), etc., upon change in temperature. A particular focus was on being able to capture the super-Arrhenius behavior that is typical in many glass-forming systems, including polymers. Consider as an example the basic Arrhenius form expression for viscosity, η , commonly called the "Andrade equation",¹³ which is given by

$$\ln \eta = \ln A + B/T, \quad [1]$$

(or equivalently, $\eta = A \exp[B/T]$) where T is absolute temperature and A and B are constants. B is often identified as an "activation energy" and associated with the related diffusive motion. In drawing a connection with free volume, Doolittle made an influential early contribution.¹⁴ In his work correlating viscosity measurements with temperature, Doolittle replaced the " T " in eq 1 with the corresponding values of "relative free volume", $(V - V_{hc})/V_{hc}$, where V is the total volume and V_{hc} the hard-core volume, yielding

$$\ln \eta = \ln A + B V_{hc} / (V - V_{hc}) \quad [2]$$

This form, referred to as the "Doolittle Equation", reflects a more complicated temperature-dependence, residing as it does in the relative free volume, rather than in the factor of " T ". While Doolittle's analysis lead him to propose this form as giving a better fit to the behavior of hydrocarbon liquids than the standard eq 1, we have found that, within the relatively high temperature range that Doolittle used, an Arrhenius form still works equally well, if not better (see note.¹⁵) A number of other models have made connections to Doolittle's early work, particularly in terms of how it invoked the concept of free volume. We will discuss this further below.

As noted above, the simple Arrhenius form (eq 1) does not capture the behavior of many glass-forming systems at temperatures approaching the glass transition. The typical situation for glass formers is that the apparent activation energy, B , (originally intended to be a constant) appears to increase as temperature decreases. This "super Arrhenius behavior" has been described by the phenomenological Vogel-Fulcher-Tamman (VFT) equation.¹⁶⁻¹⁸ The expression for the viscosity (with an analogous form for relaxation time, τ) is given by

$$\ln \eta = \ln A + B/(T - T_0) \quad [3]$$

where T is temperature, A and B are constants, and T_0 is a third constant (sometimes called the "Vogel temperature"). In this form, as T approaches T_0 the viscosity goes to infinity; fits to experimental data often show T_0 to be roughly 50 degrees below the glass transition temperature, T_g . The VFT equation is equivalent to the well-known Williams-Landel-Ferry (WLF) equation,¹⁹ which is discussed in more detail further below.

1.1 Connecting Free Volume to Glassy Behavior

It is worth emphasizing that the super-Arrhenius behavior as described by the VFT or WLF forms has provided a basic phenomenological description that tracks experimentally observed behavior in glass forming systems with reasonable success. Thus, in efforts to derive more fundamental descriptions that will yield a deeper understanding of glassy behavior, researchers have often welcomed, and even specifically targeted, models that reproduce the VFT or WLF form. However, it is important to recognize that significant differences exist in the physical details upon which the various models are based. This means that in interpreting a model's fit to its own version of a VFT or WLF-type equation it is crucial to pay attention to exactly how a quantity such as free volume has been defined within the model framework. Put another way, fitted parameters that are mapped back into each model's definitions will lead to different conclusions as to what is actually driving the physical behavior, depending on which model was chosen. Readers in the field should be aware, especially in contrasting results from different models, that the

phrase "free volume" does not always have the same meaning from one paper to the next.

An important goal of this Perspective, therefore, is to highlight the differences in how free volume is defined. Our own LCL model definition of free volume (results from which will be covered later in this paper) has an advantage of being very clearly quantifiable, as it is measured against a hard-core volume that remains fixed even as temperature (or pressure) changes. The LCL prediction for free volume therefore reflects the *maximum amount* of potentially compressible (thus "free") space available in a system. There are other models that share this definition, while a different subset involves a somewhat more nuanced view in how free volume is defined. For example, they might draw distinctions between how various contributions to the total free volume originate. It is worth the effort to clarify the differences between models, as we do below, in order to translate and make comparisons between them. This will also allow us to better place our own results in the context of earlier work.

Explicit clarification is also valuable in discussing the *approach* used to deduce the presence of, and quantify, free volume. Our method is to determine free volume first and then ask about its relationship to dynamics, rather than begin with an assumption of a particular relationship. Associated with this are the choices in the kinds of experimental properties on which any formalism must rely. For example, in probing VFT-type phenomenology, conclusions have often been drawn from analyzing dynamical data e.g. τ or η as a function of T . Note, however, that doing so involves the *presumption* that free volume is connected to dynamics and T_g . Another route is to quantify free volume via thermodynamic/PVT data; this is the path that the LCL model follows, and it presumes only that the experimental volume occupied by a sample contains within it a van-der-Waals-like 'hard core' component. The LCL theory is a statistical thermodynamic model; it does not exhibit a T_g and no formal connection with dynamic properties is assumed. Yet we show in the work

that follows that our analysis of melt behavior produces correlations that track the onset of glassiness, allowing us to develop characteristic signatures that reflect the reduction in free volume and segmental entropy characteristic of the glassy state.

1.2 Definitions for "Free Volume"

A typical free volume definition is given by the following kind of expression

$$[\text{Free Volume}] =$$

$$[\text{Total Volume}] - [\text{Some Measure of "Occupied" or "Hard-Core" Volume}]$$

where the *Total Volume* is, of course, T and P dependent, while the quantity of volume that gets subtracted may, or may not, be T and/or P dependent. For the commonly used free volume definitions see Figure 1, which shows a schematic of the contributions to free volume, and how they are related. The first differentiation concerns whether a constant *hard-core* volume, or a T -dependent volume, is subtracted from the total. The former is the most straightforward definition of free volume, and represents the maximum possible amount of free volume, i.e. everything except the limiting, fixed, hard-core contribution. We denote this simply as V_{free} , and it is given by

$$V_{\text{free}} = V - V_{\text{hc}} \quad [4]$$

In the next section we show how V_{hc} , and thus V_{free} , can be clearly calculated in the terms of our LCL model parameters, obtained by characterization using *PVT* data, since the LCL model has a natural definition for V_{hc} .

The other route to defining a free volume results in quantities that represent a portion of the "full amount". In this picture, and as shown in Figure 1, V_{free} is considered to be made up of two *types* of free volume: One is $V_{\text{free:vib}}$, which is the free space contained within the temperature-dependent "vibrational volume", V_{vib} . V_{vib} is the hypothetical volume that the segments would "own" even in the crystalline solid state, and is given by

$$V_{\text{vib}} = V_{\text{free:vib}} + V_{\text{hc}} \quad [5]$$

V_{vib} is viewed as the underlying solid-like contribution to the total liquid volume, comprised by the hard core volume (V_{hc}) plus the nearby free space ($V_{\text{free:vib}}$) expected to be covered by simple solid-like vibrational motion of the segments. Note that V_{vib} has often been called the "occupied volume" in other works in the literature, e.g. Fox and Flory.²⁰⁻²²

The other contribution to the total is the additional free volume needed to give the overall total amount 'owned' by the melt (the liquid), and we will call this the "excess free volume", denoted by $V_{\text{free:exs}}$.

$$V_{\text{free:exs}} = V - V_{\text{vib}} \quad [6]$$

Thus we have

$$V_{\text{free}} = V_{\text{free:exs}} + V_{\text{free:vib}} \quad [7]$$

In Figure 2 we present a stylized depiction of the various contributions to the total volume, with a guide to notation listed below the diagram.

The temperature dependence of the different types of free volume can be connected to the coefficient of thermal expansion $\alpha = (1/V)(\partial V / \partial T)_P$. A distinction between the "total free volume" and the "excess free volume" is that $(\partial V_{\text{free}} / \partial T)_P = V\alpha_L$, and $(\partial V_{\text{free:exs}} / \partial T)_P = (\partial V_{\text{free}} / \partial T)_P - (\partial V_{\text{free:vib}} / \partial T)_P \approx V(\alpha_L - \alpha_G)$, where α_L is that of the liquid, and α_G is that of the glass (or the crystalline solid, as it often has a similar value).

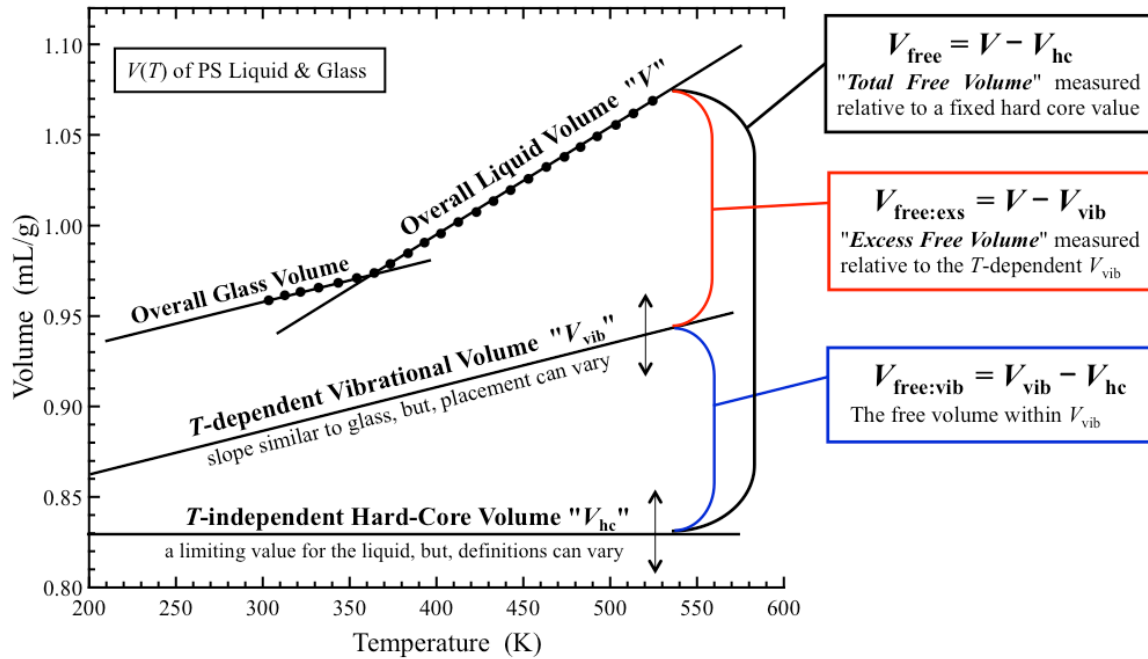


Figure 1. Diagram showing the two most common ways of defining free volume, denoted V_{free} and $V_{\text{free:exs}}$. V_{free} is the "total free volume", being the overall system volume minus a temperature independent hard-core volume, V_{hc} . $V_{\text{free:exs}}$ is the "excess free volume", being the overall system volume minus a temperature *dependent* volume, denoted V_{vib} . V_{vib} is a hypothetical amount of volume consisting of the segmental hard cores and their "nearby volume" that would be covered by simple solid-like vibrational motions. (Note that V_{vib} has often called the "occupied volume" in other works.) The amount of free volume contained within V_{vib} is denoted $V_{\text{free:vib}} = V_{\text{vib}} - V_{\text{hc}} = V_{\text{free}} - V_{\text{free:exs}}$. The T -dependence of V_{vib} (i.e. the slope of the V_{vib} line) is commonly taken to be the same as that of the glass (or solid). Details of the definitions for V_{vib} and V_{hc} have varied, and this is discussed in the text.

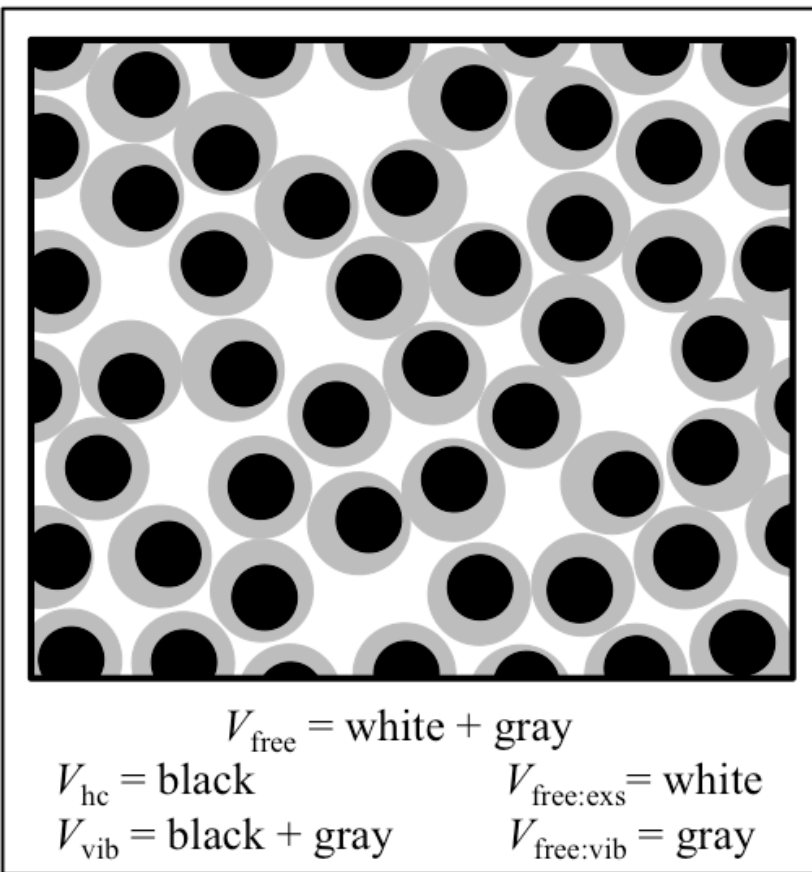


Figure 2. A diagram showing a breakdown of regions assigned to different types of volumes and free volumes in a sample of segments in a liquid. The black circles represent the hard cores of the segments. The gray regions surrounding the segmental hard cores are the (T -dependent) free space ($V_{\text{free:vib}}$) that the segments may range over when hypothetically limited to just the execution of simple solid-like vibrational motion. The white regions are the extra free space available to the segments in the liquid, above and beyond the expected solid-like range of motion. (Note, the drawing is technically not to scale for a 3d liquid, which would have a lower overall fraction of available free space, e.g. typically for a liquid, $\%V_{\text{free}} < 35\%$. Also note any remaining "space" envisioned in a representation of hard spheres at hexagonal close packing is effectively not available, so from a *PVT* relations point of view, it should thus be part of the effective hard core volume.)

It is important to be explicit about the meaning of $V_{\text{free:exs}}$ and $V_{\text{free:vib}}$. We begin with a discussion of what these quantities were intended to represent from a physical standpoint. Fox and Flory²⁰⁻²² were among those to introduce a quantity analogous to what we define here as $V_{\text{free:exs}}$, which they denoted v_f . In addition, what we identify as the T -dependent vibrational volume, V_{vib} , is analogous to what Fox and Flory denoted as the (T -dependent) "occupied volume", v_0 . The goal in identifying $V_{\text{free:exs}}$ (v_f) is to quantify that particular amount of free volume that is above and beyond the free space that would (hypothetically) be 'owned' by segments behaving in a solid-like manner. As noted above, solid-like segmental behavior reflects conditions under which the segments are restricted to smaller amplitude, solid-like, motions/vibrations and this contributes $V_{\text{free:vib}}$ to the total free volume (gray area in Figure 2). $V_{\text{free:exs}}$, that 'extra' volume associated with the larger gaps between segments in the liquid state (white area in Figure 2), is key for allowing segments to get around each other and rearrange, i.e. to behave like a liquid.

A related, and physically appealing, way to think of $V_{\text{free:vib}}$ and $V_{\text{free:exs}}$, is found in descriptions by Aharoni.²³ Here, the solid-like expansion with T – which we associate with an increase in $V_{\text{free:vib}}$ – is characterized as an increase in the free space about each segment such that the distance to its near neighbors increases, but the number of near neighbors remains fixed (e.g. expansion of a cage of fixed coordination number). On the other hand, the expansion associated with the increase in $V_{\text{free:exs}}$ with T , which Aharoni called "relocational dialation", occurs such that the distance to near neighbors remains fixed, but the number of near neighbors decreases. In the liquid, both types of expansion are imagined to occur simultaneously, while in the glass or solid, only expansion of $V_{\text{free:vib}}$ occurs.

While the quantity, $V_{\text{free:exs}}$ appears to be a useful construct, its connection to V_{vib} ($V_{\text{free:exs}} = V - V_{\text{vib}}$) makes quantitative determination a challenge. Indeed, details of how the quantity is defined vary from one treatment to another in a number of

the influential early works, and the major issue is in how the hypothetical V_{vib} is expressed as a function of T . While one might reasonably expect the slope of the V_{vib} vs. T plot to be roughly that for the glassy material, the choice of intercept, and therefore the relative position of the line (or curve), is not obvious. The line (or curve) should certainly lie below that which represents the total liquid volume, and above the constant line that describes the hard-core volume (as drawn in Figure 1). One can argue further that at lower T , the V_{vib} vs. T plot should also lie below the experimental glass line, since the glass is expected to have frozen-in packing imperfections that "waste" free space, i.e. representing space that cannot be explored through the vibrational motion of the segments. The amount of free volume that gets "frozen in" at T_g is thus the value of $V_{\text{free:exs}}$ at $T = T_g$. This amount is expected to remain fixed as T is lowered below the glass transition, since from that point on the glass will only contract by losing free space through a reduction in $V_{\text{free:vib}}$. This is analogous to the description suggested by Fox and Flory in discussing the temperature dependence of their "occupied volume", v_0 .^{20,22}

Below, we make connections between our LCL model results for the total V_{free} and the separate contributions, $V_{\text{free:vib}}$ and $V_{\text{free:exs}}$. We predict a free-volume at T_g trend that (almost) mirrors the expected T -dependence of V_{vib} (Fox and Flory's v_0), suggesting an upper bound on its location. We also resolve the $V_{\text{free:exs}}$ portion of the free volume and show it to be disappearing (that is, the distinction between the liquid and solid is disappearing, differing only by a few percent) as a melt nears its glass transition.

1.3 Connections with Widely-Referenced Early Work

In this section we outline some highlights of a number of influential earlier works. Note that historically the phrase "free volume" has been applied to both the total free volume, V_{free} , and to the excess free volume, $V_{\text{free:exs}}$ (and again, relevant to the latter, we keep in mind that V_{vib} has been called the "occupied volume"). Our LCL model quantifies the total, " V_{free} -type" of definition for free volume, and examples of other earlier works to do so include the free volume used by Doolittle,¹⁴

the free volume defined in the model of Cohen and Turnbull,²⁴ and one of the two definitions considered in Simha and Boyer.²⁵ In contrast, examples of works that defined free volume to be of the excess type, $V_{\text{free:exs}}$, were Fox and Flory,²⁰⁻²² Williams, Landel, and Ferry,¹⁹ and another definition used by Simha and Boyer.²⁵ However, even when the basic type of free volume (total or excess) is defined in the same way, dramatic differences in actual values can be seen from one model relative to another.

Simha and Boyer (SB)²⁵ defined their ($V_{\text{free:exs}}$ -type) free volume (denoted here as $V_{\text{free:exs:SB}}$) as

$$V_{\text{free:exs,SB}} = V - V_{\text{vib,SB}} = V - [V_{0,L}\alpha_G T + V_{0,L}] \quad [8]$$

$V_{0,L}$ acts here as a limiting hardcore volume ($V_{\text{hc,SB}} = V_{0,L}$), and was defined as the (linearly) extrapolated volume of the liquid down to $T = 0$. The vibrational volume, $V_{\text{vib,SB}}$, having slope, $V_{0,L}\alpha_G$, was thus pinned to this $V_{0,L}$ value. Given that their liquid $V(T)$ follows, $V = V_{0,L}\alpha_L T + V_{0,L}$, their expression for the fractional free volume becomes,

$$(V_{\text{free:exs,SB}} / V) \approx (\alpha_L - \alpha_G)T \quad [9]$$

(taking $V_{\text{hc}} = V_{0,L} \approx V$). In their analysis they observe that polymers appear to have differences in their liquid and glassy α 's, $(\alpha_L - \alpha_G)$, that are inversely proportional to their T_g values, that is, $(\alpha_L - \alpha_G)T_g = \text{constant} = 0.113$. Given that eq 9 at T_g becomes $(V_{\text{free:exs,SB}} / V)_{T_g} \approx (\alpha_L - \alpha_G)T_g$, they conclude that the fractional free volume (again, a $V_{\text{free:exs}}$ type of free volume) has a single universal value of 11.3% for all polymers at their glass transition temperatures.

There are two important discussion points that follow from their reasoning: The first is the view that all polymers have the *same* universal value of $V_{\text{free:exs}}$ at $T = T_g$, which is the amount of free volume that gets frozen into the glass for all T 's below T_g . Note that this is a much more specific statement than simply asserting *some* amount of free volume gets frozen in. In contrast, Fox and Flory (ref 22)

anticipated that $V_{\text{free:exs}}$ at T_g might vary from polymer to polymer; the concept they advanced was that below T_g a glass would be in an "iso-free volume state" (iso- $V_{\text{free:exs}}$), but that the value would not necessarily be the same for every polymer. A second point is related to the actual value for SB's predicted % $V_{\text{free:exs}}$ at T_g ; 11.3% is a fairly large amount compared to numerical values pinned in other works, such as the WLF¹⁹ approach (discussed below). Some of this difference in numerical values may be traceable to how the linear extrapolations of free volume are done. We will pursue the question of whether we expect that all polymers have the same value of $V_{\text{free:exs}}$ at T_g , (and, if so, what that value might be) below.

An excess type of free volume ($V_{\text{free:exs}}$) was also used in the influential work of Williams, Landel, and Ferry (WLF).¹⁹ Prior to making their connection with free volume they had first established their now-well-known phenomenological form, which was an expression for the ratio of relaxation times, τ/τ_{ref} ($\approx \eta/\eta_{\text{ref}}$), obtained at temperature, T , and at another reference temperature, T_{ref} . ($\tau/\tau_{\text{ref}} \approx \eta/\eta_{\text{ref}}$ is a common approximation, taking the modulus scale shift factor ≈ 1 .) The reference temperature can be taken to be T_g , and this gives the "WLF expression" in the following form

$$\ln\left[\frac{\tau}{\tau_g}\right] = \frac{-C_1(T-T_g)}{C_2+T-T_g} \quad [10]$$

As mentioned above, this result is equivalent to the VFT expression¹⁶⁻¹⁸ when one takes the ratio η/η_g , or τ/τ_g , etc. In this form, $C_1 = 17.44/\log[e]$ and $C_2 = 51.6$ K have been taken as approximate "universal constants". While these values are not truly universal, WLF had found them to apply reasonably well over a set of varied experimental systems.

As noted above, the phenomenological WLF expression tracked the observed experimental behavior, but it lacked connection with a model for the underlying physics. The link to free volume was made by showing that the above WLF

expression (eq 10) could be derived by starting with the Doolittle equation (eq 2: $\ln \eta = \ln A + BV_{hc}/(V - V_{hc})$). In the derivation, WLF noted that "fractional free volume" (free volume relative to total V) is approximately equal to "relative free volume" (free volume relative to hard-core volume, V_{hc}), and that Doolittle's constant, B , is on the order of unity; they subsequently took it to be unity. Thus, they interpreted the Doolittle equation as $\ln \eta = \ln A + 1/[fractional free volume]$, and chose a fractional free volume, $(V_{free:exs,WLF}/V)$, of the form

$$(V_{free:exs,WLF}/V) = (\alpha_L - \alpha_G)(T - T_g) + (V_{free:exs,WLF}/V)_{@T_g} \quad [11]$$

where $(V_{free:exs,WLF}/V)_{@T_g}$ is their fractional free volume at $T = T_g$, and the difference in the inverse of their fractional free volume at T , and T_g , was then equated to $\ln[\eta/\eta_g]$. Thus, $\ln[\tau/\tau_g] \approx \ln[\eta/\eta_g]$ becomes

$$\begin{aligned} \ln\left[\frac{\tau}{\tau_g}\right] &= \left[\frac{1}{(\alpha_L - \alpha_G)(T - T_g) + (V_{free:exs,WLF}/V)_{@T_g}}\right] - \left[\frac{1}{(V_{free:exs,WLF}/V)_{@T_g}}\right] \\ &= \frac{-[1/(V_{free:exs,WLF}/V)_{@T_g}](T - T_g)}{[(V_{free:exs,WLF}/V)_{@T_g}/(\alpha_L - \alpha_G)] + T - T_g} \end{aligned} \quad [12]$$

which has the WLF form of eq 10. Given that C_1 and C_2 are "approximate universal constants" applying to all systems, some conclusions follow: One is that the free volume at $T = T_g$ has the same (universal) value for all polymers, $(V_{free:exs,WLF}/V)_{@T_g} = 1/C_1 = 0.025$. Another universal value is then deduced from $C_2 = (V_{free:exs,WLF}/V)_{@T_g}/(\alpha_L - \alpha_G)$, which yields $(\alpha_L - \alpha_G) \approx 4.8 \times 10^{-4} \text{ K}^{-1}$ for all systems. WLF noted that a number of systems have a $(\alpha_L - \alpha_G)$ difference of about this value, and viewed the fair agreement as evidence that the model was reasonable.

Here we pause briefly to compare the SB and WLF free volume definitions. The WLF single universal value of fractional excess free volume at T_g (2.5%) was quite a bit smaller than the value reported by Simha and Boyer (11.3%). On the other hand, Simha and Boyer concluded that WLF's difference of $(\alpha_L - \alpha_G) \approx 4.8 \times$

10^{-4} for all systems was not particularly well satisfied. We will weigh in regarding these points when we discuss with our LCL results, below.

We observe further, that there is a fundamental difference in the WLF and SB definitions for excess free volume and for how it is handled. Even though both models use an excess ($V_{\text{free:exs}}$) type of free volume, and thus both models are similar in that the slope of the $\%V_{\text{free:exs}} - T$ plot is assumed to go as $(\alpha_L - \alpha_G)$, a contrast is that the two approaches differ *dramatically* in the placement of their curves. Simha and Boyer required, as T goes to zero, that their V_{vib} go to the liquid's extrapolated $T = 0$ value, but there is no analogous constraint in the case of WLF. Effectively, the WLF V_{vib} (though not explicitly defined) was simply anchored such that, at the point $T = T_g$ it would lie at some value below the overall liquid volume, and this anchoring point (effectively placing V_{vib} 2.5% below the total volume) was simply determined by the dynamics data (the WLF fit). The effective anchoring of V_{vib} near $T = T_g$ does have an advantage of staying near the experimental data range and thus avoids the need to perform a long linear (and thus questionable) extrapolation to $T = 0$. On the other hand, the WLF definition was not strongly tethered to actual volumetric data.

Another important distinction is the following: WLF introduced an excess type of free volume ($V_{\text{free:exs}}$) into Doolittle's equation (eq 2), however, Doolittle originally advanced his form based on the use of a total free volume ($V_{\text{free-type}}$). That is, Doolittle characterized free volume relative to a T -*independent* hard-core volume; he took $V_{\text{free}} = V - V_{\text{hc}}$, where the fixed V_{hc} values were determined by extrapolating the $V(T)$ data (and incorporating realistic curvature) down to $T = 0$. While the WLF expression, using their $V_{\text{free:exs}}$ -type fractional free volume, appears to work reasonably well (e.g. it does follow the form of the dynamics), one might argue that the way in which they introduce free volume is inconsistent with Doolittle's intended definition. *The discrepancy is fundamental:* a form for (fractional) free volume intended to have a temperature dependence $((\partial V_{\text{free:exs}} / \partial T)_P / V)$ that goes as the difference $(\alpha_L - \alpha_G)$ was substituted into an

expression that was instead advanced assuming a free volume form having a temperature dependence $((\partial V_{\text{free}}/\partial T)_P/V)$ that goes as α_L , alone. Furthermore, Doolittle's free volume did not go to zero at finite T , while WLF's defined theirs such that it does. This raises the question: Which type of free volume definition (V_{free} or $V_{\text{free:exs}}$) *should* be applied in the Doolittle equation? We will come back to this question in the context of discussing our own results.

There have been other influential works, two particular examples of which are the free volume models of Cohen and Turnbull²⁴ and Cohen and Grest.²⁶ Free volume was defined in the Cohen and Turnbull work as being the total thermal expansion at constant P (relative to a T -independent van der Waals volume contribution) and thus was a V_{free} -type of free volume definition. The free volume in Cohen and Grest was more complex but reduced to the Cohen and Turnbull free volume form at higher temperatures. Also, the Cohen and Grest model, having an additional (fourth) parameter, was able to fit dynamics data over a wider temperature range. However, the corresponding (dynamically-fitted) volumetric behavior of the model did not agree very well when compared with the actual volumetric data for the systems tested,²⁶ and this was also found to be the case in later studies by other researchers.^{9,27} The simpler Cohen and Turnbull model will be described briefly below.

Cohen and Turnbull, noting the wide use of the form of the phenomenological Doolittle equation, presented a derivation. They focused on diffusion, outlining a picture of molecular transport as occurring when molecules move into voids of some critical size (denoted " v^* ") or greater. They identified the creation of these voids as arising from redistribution of system free volume. They solved for the probability distribution of void sizes by considering the maximum number of ways of distributing free volume throughout the system under the constraints that the total system free volume ($V_{f,CT}$), and total number of molecules (N_{CT}), are conserved. Integrating over this distribution (from v^* to ∞) resulted in the probability of finding

a void of size v^* or greater, given by $P(v^*) = \exp[-\gamma^* N_{CT}/V_{f,CT}] = \exp[-\gamma^*/v_{f,CT}]$, where $v_{f,CT} = V_{f,CT}/N_{CT}$ was their average free volume per molecule, and γ is a constant. With the diffusion coefficient being (approximately) proportional to $P(v^*)$, the viscosity was taken as proportional to $1/P(v^*)$, i.e., $\eta \propto \exp[\gamma^*/v_{f,CT}]$, and this yielded the Doolittle form. In applying the form, η is then a function of $v_{f,CT}$, with γ^* being a parameter.

Up to the point of obtaining the Doolittle equation, v^* and $v_{f,CT}$ were general quantities, in the sense that no form was given for $v_{f,CT}$ as a function of temperature. As noted above Cohen and Turnbull then defined their free volume ($v_{f,CT}$) to be the total thermal expansion at constant P above a T -independent van der Waals volume ($v_{0,CT}$). This ultimately lead to the approximate form, $v_{f,CT} \approx \alpha \langle v_{m,CT} \rangle (T - T_0)$, where $\langle v_{m,CT} \rangle$ was the mean molecular volume; and T_0 was defined to be a temperature at which the free volume disappears (where the volume equals $v_{0,CT}$). Substitution into the Doolittle form yielded $\ln \eta \sim \gamma^*/v_{f,CT} = \gamma^*/[\alpha \langle v_{m,CT} \rangle (T - T_0)]$. This result was shown to be effective in fitting experimental viscosity and diffusion data, with γ^* and T_0 used as fitting parameters.

While the Cohen and Turnbull free volume was defined to be the total thermal expansion ($v_{f,CT}$ is a V_{free} type free of volume measured against a hard-core), it might therefore seem a bit presumptuous to insist that there is some (finite) temperature, T_0 , at which this free volume disappears. In other words, the assertion is that the total volume reaches the hard-core volume at finite T . However, this feature in the temperature dependence of $v_{f,CT}$ is absolutely essential in fitting to the data.

Here we wish to emphasize the following: *Any function for free volume having the form $\{T - [\text{constant}]\}$ can lead to the VFT form.* Cohen and Turnbull's free volume, $v_{f,CT}$, is a function going as T minus a constant. When substituted into the Doolittle form it yields an expression capable of fitting experimental data. WLF also

substituted their particular definition of free volume into the Doolittle form, and that was also shown to fit the data. However, the WLF free volume definition differed in being based on an excess ($V_{\text{free:exs}}$) type of free volume. It was not intended to capture the total expansion, being rather, $(\alpha_L - \alpha_G)(T - T_g)$ plus a small amount (0.025 at T_g). Two apparently very different models each evidently can fit the experimental data. In fact, in terms of their T -dependence they are *not* so different, in that that the WLF free volume, like the Cohen and Turnbull definition, goes as T minus a constant. (This is so because $0.025 < 0.00048 \times T_g = (\alpha_L - \alpha_G)T_g$ for any $T_g > 52\text{K}$.) When this kind of temperature dependence is substituted into a Doolittle-type equation it is guaranteed to produce the VFT form, and thus be able to track the experimentally observed super Arrhenius behavior.

So, can we say *definitively* that free volume is intimately related to T_g and super-Arrhenius behavior? The evidence for such a connection can only be convincing if it is analyzed without presuming a connection in the first place. While this statement seems obvious, we believe that somewhat circular reasoning does exist in using some of the models described above to analyze dynamical data. In this sense, the LCL model may offer an advantage in that free volume values, however the free volume is defined, must be directly linked to experimental volumetric results. In extracting free volumes by applying a derived equation of state to experimental data on the liquid/melt, or solid/glass, we therefore avoid any assumptions regarding how dynamic properties are linked to free volume.

1.4 Overview of the Remainder of this Article

In the following sections we shift to focusing on results from our own free volume analysis using the LCL model. In the course of doing so we will frequently reference the issues discussed above. In addition, we will explore a close connection between our free volume results and the LCL theory's prediction for the entropy per theoretical segment. The ability to model and analyze entropy is important because

it creates bridges between the LCL model and a number of entropy-related concepts and theories that have been widely applied in the study of glassy behavior. For example, entropy is a central quantity in the Adam and Gibbs theory¹² and we connect to this approach in the upcoming discussion.

The results we present focus on constant (ambient) pressure. There has been criticism of earlier models based on a "free volume only" point of view because of a failure to explain pressure dependent data.¹⁻⁹ Whether or not pressure is fixed, our observation is that free volume plays an important role. However, the effect of changing temperature cannot be ignored, even when the volume is fixed. The discussion below will thus reflect the intrinsic view that accounting for both temperature and free volume will be essential in order to make connections with the more general, P -dependent dynamics data. This is a direction we are currently pursuing.

The connections we do make here to experimental dynamic properties are restricted to data at the glass transition, T_g . Among reasonable (but still somewhat arbitrary) definitions, T_g is typically taken to be the temperature at which $\tau = 100$ seconds, or $\eta = 10^{13}$ poise. These dynamical T_g 's are expected to be reasonably close to the corresponding measures of T_g determined by dilatometry or by calorimetry (the source of most of the experimental values to which we compare). As a side note, we observe this means that any analysis of fragility^{28,29} (essentially a measure of the shape of the functions, $\tau(T)$, $\eta(T)$) will lie outside the present scope of our results and discussion. Though comparison is made with experimental dynamics data just at the point, $T = T_g$, the analysis of the corresponding model *thermodynamic* properties is much broader and encompasses T -dependent behavior in the melt.

In addition to our LCL model there are a number of other physics-based equations of state designed for chain molecule fluids that are commonly used. The interested reader can find several examples in ref 30 and references therein.

Furthermore, recent modeling reviews in refs 31 and 32 cover examples of theories of glass forming systems that are not necessarily equation of state or free volume-based. Though a detailed background is beyond the scope of the paper we note some examples where polymer equations of state have been applied to the study of glassy behavior and/or free volume. One is the generalized entropy theory (GET),³³⁻³⁵ which makes use of the lattice cluster theory equation of state (LCT)^{36,37} of Freed and coworkers, combined with the theory of Adam and Gibbs.¹² Another example is the Simha and Somcynski (SS) equation of state,^{38,39} which has been employed in attempts to quantify free volume from *PVT* data analysis; refs 40-47 show some applications such as correlating viscosity (e.g. linking with Doolittle-type eqns), relaxation times, and conductivity, and also interpretation of positron annihilation lifetime spectroscopy (PALS) studies.

It is worth noting that in the SS equation of state separate contributions may arise from two types of free volume. The model incorporates segments in compressible cells along with unoccupied cells (holes). The free volume contribution from the former would be the solid-like $V_{\text{free:vib}}$ and from the latter (the holes) would be the excess free volume, $V_{\text{free:exs}}$. However, although the model fits the overall *PVT* data well, the relative weighting from the two underlying free volume contributions does not seem to provide a good qualitative representation of the separation of the solid-like and excess expansion behaviors. It appears that the thermal expansion of the cells is too weak to represent a solid-like contribution; this will be discussed in more detail below. In contrast, the LCL model applies a more simplified coarse-grained definition of free volume (the overall V_{free}), and it yields convenient closed-form analytic expressions for the thermodynamic functions. To our knowledge the study presented here is unique, wherein the same model has been consistently applied to characterize a sizeable sample of polymers and used to predict free volumes (and other thermodynamic properties), which are then related to experimental glass transition temperatures.

2. Theory

The Locally Correlated Lattice model is not a "free volume model"; rather, it is a model that can be used to calculate free volume. The LCL theory embodies a first principles, molecularly based, thermodynamic treatment. In previous work we have derived and used the LCL equation of state, $P(N,V,T)$, to analyze *PVT*-type data en route to calculating many thermodynamic (e.g. energetic, entropic) properties, both for pure fluids and mixtures.⁴⁸⁻⁵² Fitting to a limited set of experimental data, we obtain molecular level information that is transferable to the calculation of other properties, or at other conditions, for which no data may be available. Most recently, we have used *PVT* results to make connections between experimental volumes and the corresponding underlying free volumes for a wide variety of polymer systems.^{10,11} (Some preliminary results connecting $\%V_{\text{free}}$ to T_g were presented ref 10). The LCL molecular level characterization leads to a simple and well-defined route to molecular hard-core volumes, which allows the calculation of free volumes. Furthermore the molecular parameters lead to a characteristic theoretical segment, allowing us to quantify and compare properties on a "per-segment basis", which, can be quite revealing. We pursue this further in the section on Results.

The LCL model is based on a picture of a compressible fluid of chain-like molecules. "Compressible" means that there is free volume, all of which is contained in sites that are unoccupied (see Appendix). For a one-component system there are three molecular parameters: r , the number of segments (not to be interpreted as the number of chemical repeat units) per molecule, v , the temperature-independent hard-core volume of a segment, and ε , the nonbonded near neighbor segment-segment interaction energy. We obtain a fundamental expression for the Helmholtz free energy, A , as a function of the number of molecules, N , volume, V , and temperature, T , and from $A(N,V,T)$, all other thermodynamic properties can be derived using standard thermodynamic relationships. (The symbol, A , was used differently above to represent the pre-exponential factor in the dynamics expressions,

but the different uses should be clear in the context.) More information on the model is available in the appendix and from refs 48 and 49.

The LCL model expression for the pressure, $P = -(\partial A / \partial V)_T$ is given by

$$\frac{P}{k_B T} = \left(\frac{1}{v} \right) \ln \left[\frac{V}{V - Nrv} \right] + \left(\frac{3}{v} \right) \ln \left[\frac{V - (Nv/3)(r-1)}{V} \right] - \left(\frac{3}{v} \right) \left(\frac{(2r+1)^2}{(V/Nv) - (1/3)(r-1)} \right) \left(\frac{\exp[-\varepsilon/k_B T] - 1}{(1/3)(2r+1)\exp[-\varepsilon/k_B T] + (V/Nv) - r} \right) \quad [13]$$

which is written as a function of N , V , T (k_B is Boltzmann's constant). Eq 13 shows how the molecular parameters, r , v , ε , appear in the equation of state. For the purposes of this study we have determined the characteristic molecular parameters for 51 different polymer melts by fitting eq 13 to the corresponding *PVT* data. An example showing the resulting *PVT* fitted model curves for the case of polystyrene will be covered as we discuss results below. More details are available in the appendix, which includes a table of the parameter values, references for *PVT* data,^{30,53-59} and references for experimental T_g data.^{53,56,58,60-72}

Our LCL prediction for the hard-core volume using the LCL model is straightforward, being $V_{hc} = Nrv$. The hard-core volume is simply the number of molecules, multiplied by the number of segments per molecule, multiplied by the T -independent hard-core volume per segment. Thus, the LCL free volume is given by the difference between the (experimentally-fitted) total volume of the sample (V) and the hard-core volume

$$V_{\text{free}} = V - Nrv \quad [14]$$

Note that the *fractional* free volume, V_{free}/V , is usually the relevant reduced quantity that is insightful for comparison. We typically quote, tabulate, and plot our fractional free volumes as percentages, and $\%V_{\text{free}}$ is given by

$$\%V_{\text{free}} = 100 \times (V - Nrv)/V \quad [15]$$

As we have been noting, since the LCL model's V_{free} (and $\%V_{\text{free}}$) is measured against a T -independent hard-core, it therefore represents the "total amount" of free volume. The excess free volume, $V_{\text{free:exs}}$ ($= V - V_{\text{vib}} = V_{\text{free}} - V_{\text{free:vib}}$) is contained *within* our computed V_{free} . Below we discuss the way in which our results allow us to deduce something about the relative contribution from $V_{\text{free:exs}}$.

3.0 Results and Discussion

3.1 LCL Predictions for V_{free} at T_g for a Large Set of Polymers

We first show that the LCL model predicts a strong connection between polymer free volume and T_g , and then discuss some trends in behavior as revealed by our analysis. It is important to emphasize that we do not *assume* any *a priori* connection between free volume and T_g and, further, that the LCL model does not exhibit a glass transition; there are no discontinuous changes in any thermodynamic quantity or its derivative(s) with temperature. So, for example, as the system temperature decreases below the experimental T_g , the model melt (liquid) simply shows a smooth continuation of properties in the super-cooled equilibrium liquid regime. The T_g values that we quote are thus the experimental values taken from the literature.^{53,56,58,60-72} In modeling the equilibrium liquid state, the molecular characterization via which we obtain values for r , v , ε has been based on fitting corresponding equilibrium melt *PVT* results. While we focus on the analysis of polymers in their liquid state, we have also had occasion to use literature *PVT* data (from the same source as the melt data) collected on some few glassy samples. This involves a separate analysis, yielding a different set of parameters and is discussed further below. In the appendix more detailed comments are given on distinctions between melt and glassy data; we note here that in using the glassy data one assumes an effective quasi-equilibrium state.

As noted above we consider a sizeable set of 51 polymer melts and these are tabulated in the appendix. This set covers a range of chemical diversity, including simple hydrocarbon polymers (e.g. polyolefins and polydienes), polystyrenes, polyethers, polyacrylates, polymethacrylates, and others containing flourine, chlorine, hydrogen bonds, rings in the backbone, etc. The glass transition temperatures span from 149 K (poly dimethyl siloxane) to 490 K (poly ethersulfone). In addition, although we do not analyze fragilities, a wide range is represented as well, with polyethylene and poly(n-hexyl methacrylate) as examples at relatively low fragility (for polymers), and polymethylmethacrylate and polyvinylchloride at high fragility.

In our analysis we first focus on V_{free} of the melt at temperatures greater than and equal to the experimental glass transition temperature, T_g . Using eq 13 for $P(N,V,T)$ along with eq 15 we generate a prediction for the $\%V_{\text{free}}$ as a function of T for each polymer in our sample of 51 polymers. Three examples of $\%V_{\text{free}}(T)$ curves are shown in the upper panel of Figure 3 for the cases of PBA (polybutylacrylate), PS (polystyrene), and TMPC (tetramethyl bisphenolA polycarbonate). At any given temperature we predict that PBA has the highest $\%V_{\text{free}}$, followed by PS, then TMPC (lowest $\%V_{\text{free}}$). Experiment shows that PBA also has the lowest experimental T_g , with that for PS being higher, and the highest for TMPC. This agrees with the pattern we have repeatedly found, viz. that when $\%V_{\text{free}}$ values, calculated at the same, fixed, temperature are compared within a set of polymers the ranked values are in the inverse order as the set of experimental T_g values.^{10,11}

However, a fixed T is not the "same" temperature for each polymer, since it will be a varying distance from that polymer's glass transition temperature. Thus, comparing LCL predictions for $\%V_{\text{free}}$ at a polymer's glass transition (which involves extrapolating the theoretical $\%V_{\text{free}}(T)$ curve to temperatures at the lower bound of the melt regime) represents what might be considered a more even footing. LCL predictions for $\%V_{\text{free}}$ at $T = T_g$ are marked as symbols in the upper panel of Figure 3. Returning to the set of polymers described above, the $\%V_{\text{free}} (T = T_g)$ ordering now

goes as PBA < PS < TMPC. That is, PBA drops to the lowest $\%V_{\text{free}}$ at T_g ; TMPC drops the least before going glassy. The three points (PBA, to PS, to TMPC) for $\%V_{\text{free}}$ at $T = T_g$ appear to form a line as T_g value increases, and we find that this pattern is generally maintained when we consider the full sample of polymers.

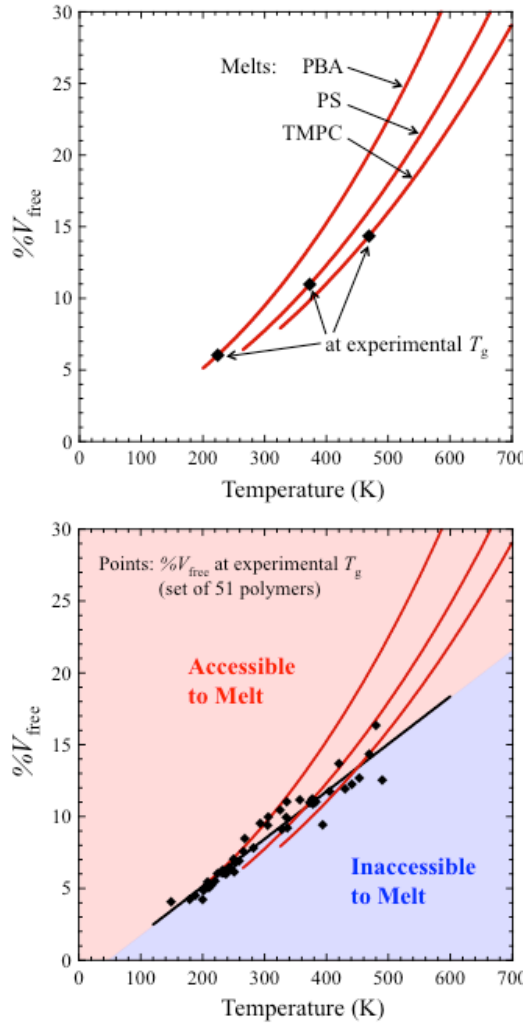


Figure 3. Trends in polymer free volumes, in the melt, and at their experimental T_g . The upper panel shows curves of $\%V_{\text{free}}$ as a function of T for three polymers chosen as examples: PBA, PS, and TMPC. The symbols on each curve mark the $\%V_{\text{free}}$ value at that polymer's experimental $T = T_g$ value. The lower panel shows the full set of points marking $\%V_{\text{free}}$ at the experimental T_g for each of the 51 polymers in our sample set, along with the same example melt curves (PBA, PS, TMPC) from the above panel. The trend in $\%V_{\text{free}}$ at T_g vs. T_g marks an average boundary (drawn as the heavy black line, correlation coefficient = 0.968) which separates the region accessible to melts from the region where they are not observed. The boundary is thus a prescription for the T -dependent minimum amount of free volume that a polymer must have for it to still be in the melt state.

3.2 A T -Dependent Boundary of Minimum $\%V_{\text{free}}$

The lower panel of Figure 3 shows the points marking the value of $\%V_{\text{free}}$ at $T = T_g$ for the full set of 51 polymers, these values all being determined in the same way as described above, by following the predicted $\%V_{\text{free}}(T)$ curve down in temperature to its value the experimental T_g . There is a clear linear trend of $\%V_{\text{free}}$ at $T = T_g$ increasing with T_g and we have marked the pattern with a corresponding best fit line (correlation coefficient = 0.968). The melt curves (three are shown, but the appearance is similar for all) are steeper than the line, and their intersection with this line represents a route to predicting T_g by proposing this as a criterion for where the super-cooled melt will fall out of equilibrium and become a glass. In effect, the line acts as a T -dependent boundary of minimum free volume; a polymer must have at least this minimum amount of $\%V_{\text{free}}$ for it to still be in the equilibrium melt state.

Obviously, the points — which give the LCL predictions for $\%V_{\text{free}}$ values at $T = T_g$ — are somewhat scattered about the line. If all polymers went glassy exactly at the $\%V_{\text{free}}$ boundary line, then all of the points would be located perfectly on the line, which is not the case. However, the trend is still robust enough that we expect it should be reasonably predictive. As a test, we have determined the temperatures at which the $\%V_{\text{free}}$ curve of each of the polymer melts intersects the best fit line, and then compared our predicted T_g with experimental values. (The Supporting Information includes a plot of all the predicted vs. experimental T_g 's.) We find that the predictions show an average absolute deviation from the experimental T_g values of 51.2 K. To place this in context, this variability is fairly small compared to the span of experimental T_g 's of the polymers in the sample set, which ranges from $T_g = 149\text{K}$ (PDMS) to 490K (PES) and thus covers 341 degrees. The predictions therefore deviate by about 15% of this total possible range. This leads us to conclude that there is a strong fundamental contribution to glassification coming from free volume-based considerations of the *melt* sample. We know the molecular characteristics such as chain stiffness, fragility, detailed atomistic interactions, etc. come into play in glassy behavior, so it is perhaps surprising to discover that such a

simple coarse-grained thermodynamic model of the melt state is able to capture something about the incipient glass within.

3.3 Connections with Simha and Boyer and with Doolittle

We can now make comparisons with some of the free volume results from the work mentioned in the Introduction, for example Simha and Boyer.²⁵ These authors actually presented two free volume definitions; the one described above was an excess free volume ($(V_{\text{free:exs,SB}}/V) \approx (\alpha_L - \alpha_G)T$). The other, drawing its origin from earlier studies,⁷³ would be categorized as a definition for total free volume, $V_{\text{free,SB}}/V = (V - V_{0,L})/V \approx \alpha_L T$. Recall that their proposed pattern of $(\alpha_L - \alpha_G)T_g \approx \text{constant}$ would imply a universal value of (the excess) $\%V_{\text{free:exs,SB}}$ at T_g . Consequently, the alternative proposed pattern of $\alpha_L T_g \approx \text{constant}$ would imply a single universal value for (the total) $\%V_{\text{free,SB}}$ at T_g . SB's total free volume, $\%V_{\text{free,SB}}$, is the natural quantity against which our own results can most easily be compared. Recalling our $\%V_{\text{free}}$ results from Figure 3, we clearly do not predict a universal constant for $\%V_{\text{free}}$ at $T = T_g$. In addition, given that SB assumed there would be a linear T -dependence of $V_{\text{free,SB}}/V$ all the way to $T = 0$, we expect that $\%V_{\text{free,SB}}$ values at other temperatures will be much larger than the LCL predictions, which account for positive curvature in $V(T)$. For example, near T_g , $\%V_{\text{free,SB}}$ results appear to be roughly twice our corresponding predicted values. The SB values for *excess* free volume are also large; recall from our remarks above that they were large compared to WLF's excess free volume values. In fact, SB values for the *excess* free volume can be larger than our results for the *total* $\%V_{\text{free}}$. This is evident by noting that at T_g the excess $\%V_{\text{free:exs,SB}} \approx 11.3\%$, while our LCL model estimates that at T_g , we expect *total* $\%V_{\text{free}}$ to be near 11.0% for a polymer like PS, and thus even lower for many other polymers (Figure 3).

Aharoni²² also concluded that the SB estimates of $\%V_{\text{free}}$ appeared to be unreasonably large. When substituted into the Doolittle equation (eq 2, taking A on the order of 1 poise, and B , in accordance with Doolittle, on the order of unity) he

pointed out that $\%V_{\text{free:exs,SB}}$ of 11% at T_g would predict a viscosity of about 9000 poise, far below the expected value, which would be around 10^{13} poise at T_g . Note further that this involves substituting the SB *excess* fractional free volume into an equation that Doolittle originally intended for the input to be *total* fractional free volume (technically the total relative free volume). In fact using SB's total percent free volume would yield viscosity values that would be even lower than 9000 poise at T 's near T_g . Here we should observe that our own LCL total percent free volumes ($\%V_{\text{free}}$) substituted in this way into Doolittle's equation ($A = 1$ poise, $B = 1$) would also, not be expected to give reasonable viscosity values near T_g . As an example, for PS our prediction for $\%V_{\text{free}}$ is 11%, and used in Doolittle's equation (again) would predict a much-too-low viscosity of 9000 poise.

Part of the explanation for the above extremely low viscosities appears to be in using a B value of unity. Although it is well known that WLF used this for B , it is not at all conclusive that B should remain constant from system to system. Doolittle reported $B = 0.9995$ for n-heptadecane, which was the only system value he quoted.¹⁴ However, we have generated plots¹⁵ using his own tabulated results and found optimized B values to vary from 0.69 (C7) to 1.34 (C64). These deviations from unity will have significant impact on the viscosity values, because they operate in the exponential. A related question is to ask is how reliable the WLF free volumes can be if they were calculated using $B = 1$? A small shift to a different value of B will significantly change the calculated viscosity, and thus the implied free volume. In a recent example, Sorrentino and Pantani,⁴⁷ using the Simha and Somcynski equation of state, also predicted fractional free volumes for PS in the range of 11 to 13% and did manage to fit the Doolittle equation to the experimental viscosity values (in the vicinity about 10^5 poise) in the T -range of 450 – 500K, but only by using $B = 1.62$. Though the fit was demonstrated to be adequate in the 10^3 to 10^5 poise range, those viscosities are still many orders of magnitude smaller than values expected at temperatures closer to T_g , which are on the order of 10^{13} poise. It seems likely that for the Doolittle form to continue to hold up into lower T 's a T -dependent B might be required.

We have come to the conclusion that a key issue concerning application of the Doolittle equation has to do with the temperature range of interest. It is useful to note that the VFT type equation is known to be effective over only a *limited* range of T . Thus one VFT parameter set might cover a region of about T_g to say, 100 degrees above T_g , then from this "crossover temperature" T_B (\sim 10-50% above T_g) starts another non-Arrhenius regime where another VFT parameter set would be needed, then above this (above a temperature, " T_A ") is the Arrhenius regime. (e.g. see refs 1,2,74,75) Doolittle's work on hydrocarbons covered a rather high temperature range (e.g. about $T = 300$ to 570K for n-heptadecane) compared to their expected T_g 's (e.g. expected to be well below 150K^{76,77}), and this seems to be a reason for why we also observed¹⁵ that the Arrhenius form for viscosity applies just as well on Doolittle's data. On the other hand, many polymeric studies (particularly those focused on glassy behavior) have often involved ranges much closer to the system T_g . The pattern seems, that models that made use of Doolittle's original implementation as the phenomenological justification for connecting viscosity and free volume, but, were still applicable near T_g , were ones that had substituted forms for free volume that were capable of going to zero at finite T (e.g. T minus a constant, to give the VFT form, as in WLF and Cohen and Turnbull). By contrast, Doolittle's free volume's went smoothly to zero at $T = 0$.

3.4 Information from Modeling both Melt and, Glass

It would be useful for us to connect LCL predictions for *total* $\%V_{\text{free}}$ with values of *excess* free volumes ($\%V_{\text{free:exs}}$) that are provided in other works. In undertaking this translation we focus on the properties of one particular polymer, PS, because there exist sufficient data for both the glass and melt states from a single source.⁵³ We therefore feel confident in being able to accomplish an internally consistent characterization of both melt and glass. Note, again, that the LCL model does not exhibit a glass transition and, since we are dealing with PS in two states, two, separate, analyses are involved: one of the equilibrium melt data and one of the

glass data. Here we view the glassy data we parameterize as representing an effectively quasi-equilibrium state; additional remarks may be found in the appendix. As we would expect, the characteristic parameter values are different for the two states (melt vs. glass). Recall our expectation, in line with the picture of Fox and Flory^{20,22}, that a glass will have some excess free volume "frozen in", and that this portion will not participate in the glass's expansion/contraction behavior upon changes in T and P . (As an aside, we note that while a glassy sample does lose frozen-in free volume as it slowly ages, a static condition of quasi-equilibrium is typically assumed on a practical time scale.) We anticipate that the LCL parameters for the glassy hard-core volume, rv , will reflect this frozen-in free volume, and thus be *larger* than the corresponding predicted hard-core volume of the melt. Put another way, if, frozen-in imperfections cause a waste of free space such that it cannot be accessed upon compression, then it is sensible to imagine that this space is effectively "hard" from a PVT relations standpoint and thus should be added to the amount that was already reporting as "hard" in the melt.

The results for the LCL model fit to the PS glassy and melt data are shown together in Figure 4. The model curves and data are plotted in the form of specific volume as a function of T , in isobars at six pressure values from 0 (\sim atmospheric pressure) up to 100 MPa. The LCL values for the product rv , are marked below the sets of glass and of melt curves. The melt rv value, 0.8718 mL/g, is the molecular hard core volume we have used to obtain V_{hc} and is reflected in the values shown earlier in this paper for V_{free} .

Turning to the glassy state analysis, the effective rv is indeed larger (0.9133 mL/g) than the value obtained for the melt. The difference in rv between the two fits is 0.0415 mL/g, amounting to $\sim 4.2\%$ of the total volume, and this can be interpreted as the LCL prediction for the excess free volume that gets frozen into the glass; this value will remain fixed for all temperatures below T_g . Referring back to Figure 2, we still interpret rv_{melt} as the hardcore volume V_{hc} , represented by the

black regions. However, rv_{glass} contains the additional volume associated with the extent to which the molecules are inefficiently packed at the glass transition. A visual representation of rv_{glass} would therefore comprise all the black region plus that portion of the white region that survives when T falls to T_g . In other words, in Figure 2, at the glass transition, the difference, $rv_{\text{glass}} - rv_{\text{melt}} = 0.0415 \text{ mL/g}$ is the volume that gets stuck due to inefficient packing, represented by the surviving white region, i.e. the excess free volume at T_g .

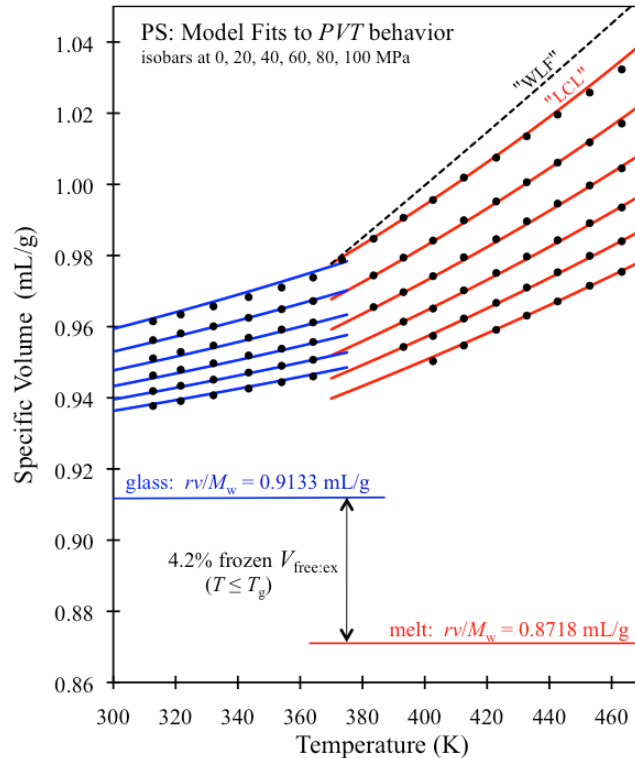


Figure 4. LCL model fitting to the PVT properties of both polystyrene (PS) melt and glass. Results are plotted in the form of $V(T)$ isobars (specific volume) at pressure values of 0, 20, 40, 60, 80, and 100 MPa. The red curves are the LCL $V(T)$'s fitted to the PS melt, and the blue curves are LCL $V(T)$'s fit to the PS glass, and the points are the experimental data taken from ref 53. The values of the fit parameters rv are marked; $rv = 0.8718$ and 0.9133 mL/g for melt and glass respectively, and the difference in these values leads to an estimated 4.2% of excess free volume at $T = T_g$. Also shown for comparison is a dashed curve showing the $V(T)$ ($P = 0$ isobar) for the WLF model ($(\alpha_L - \alpha_G) = 4.8 \times 10^{-4} \text{ K}^{-1}$) where α_L is deduced using the α_G from the LCL fit to the PS glass.

3.5 Comparing with Excess Free Volumes of WLF

Using the information from parameterizing both the melt and glass states of PS we can now estimate an LCL excess free volume, which will allow us to make connections with WLF results (eq 11). First, we consider the value of excess free volume at T_g . As noted above, we have obtained for our one test case of PS an excess free volume of 4.2%. This can be compared with the often-quoted WLF universal value of $\%V_{\text{free:exs,WLF}} = 2.5\%$. The LCL estimate is somewhat higher than the WLF value, but much closer to it than the excess free volume of Simha and Boyer, $\%V_{\text{free:exs,SB}} = 11.3\%$.

As discussed in the Introduction, the WLF equation for the temperature dependence of the fractional excess free volume (eq 11) yields a line anchored to the value at $T = T_g$ (2.5%) and has a fixed slope of $(\alpha_L - \alpha_G) = 4.8 \times 10^{-4} \text{ K}^{-1}$. Our fit to the PS glass data in Figure 4 yields $\alpha_G = 2.6 \times 10^{-4} \text{ K}^{-1}$ which would result in a WLF prediction for α_L of $7.4 \times 10^{-4} \text{ K}^{-1}$. This can be compared to the result from the LCL fit to the experimental PS melt, which yields $\alpha_L = 6.2 \times 10^{-4} \text{ K}^{-1}$.

We can now produce a WLF-based prediction for the corresponding zero pressure (\sim atmospheric) $V(T)$ isobar, anchoring it to the specific volume at T_g , and using the WLF α_L value obtained above. The result is given as the dashed curve in Figure 4, and it shows considerable departure from the experimental data. In other words, for this case of PS, given an accurate value for α_G the WLF model somewhat overestimates α_L . Simha and Boyer²⁵ had compiled a table of value of $(\alpha_L - \alpha_G)$ values for polymers and inspection of these values shows they have an average of $4.81 \times 10^{-4} \text{ K}^{-1}$, which is very close to the WLF universal value of $4.8 \times 10^{-4} \text{ K}^{-1}$. However, SB were critical of the WLF universal $(\alpha_L - \alpha_G)$ applying for all polymers, likely because of the variability they observed within the table. Indeed, the standard deviation of the $(\alpha_L - \alpha_G)$ values in the SB table is almost 50% ($2 \times 10^{-4} \text{ K}^{-1}$), even larger deviation than the single case of PS detailed here.

3.6 The $\%V_{\text{free}}$ Boundary, $\%V_{\text{free:exs}}$, $\%V_{\text{free:vib}}$: Piecing It All Together

We return to a discussion of the correlation in Figure 3 that showed $\%V_{\text{free}}$ at T_g increasing roughly linearly with T_g of the system. We have interpreted the trace of the $\%V_{\text{free}}$ at T_g points as a boundary of minimum $\%V_{\text{free}}$, below which melts are not observed. More specifically, we regard the boundary line as delineating the condition such that, as T decreases, a melt $\%V_{\text{free}}$ curve would be approaching solid-like behavior. Here we present a rationale for such an interpretation.

Consider the following: From the values tabulated in Simha and Boyer,²⁵ the average α_G of the polymers is $2.2 \times 10^{-4} \text{ K}^{-1}$ (with standard deviation = $0.7 \times 10^{-4} \text{ K}^{-1}$). Using this value for the slope we produce a plot, indicated as a blue dashed line, in Figure 5 that is anchored at $\%V_{\text{free:vib}} = 0$ at the $T = 0$ origin and interpret that to represent how $\%V_{\text{free:vib}}$ changes as T increases. Recall that $\%V_{\text{free:vib}}$ is denoted by the gray area of the accompanying schematic. The increase in gray area with T correlates with the temperature-dependence of segmental vibration.

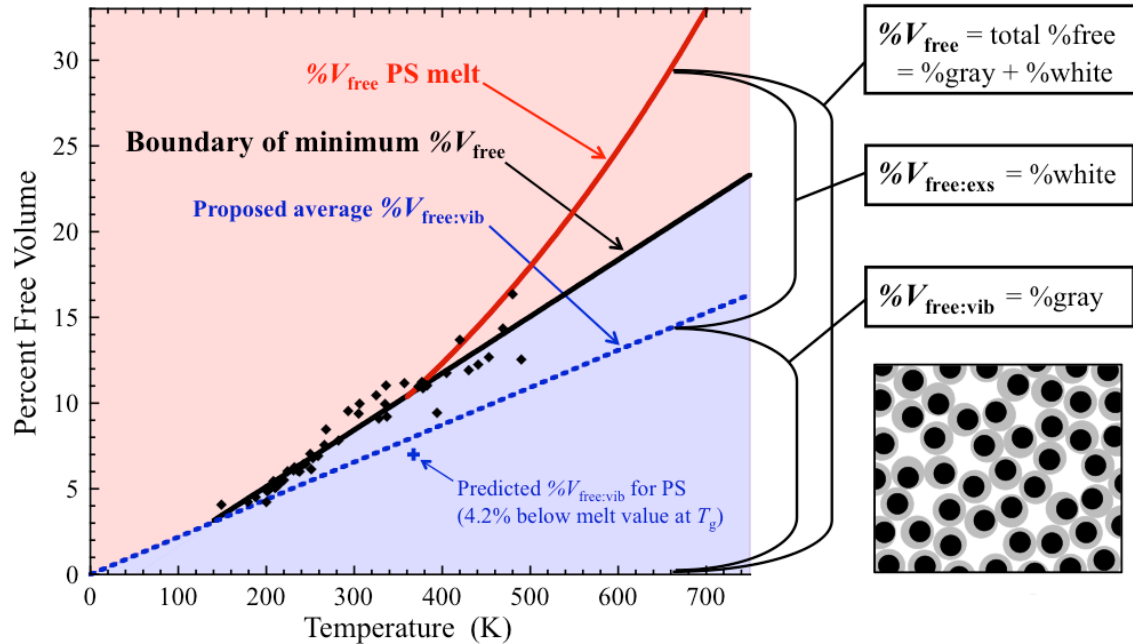


Figure 5. The boundary of minimum total $\%V_{\text{free}}$ (black line) depicted together with a proposed location for $\%V_{\text{free:vib}}$ (dashed blue line) and a corresponding quantification of excess free volume, $\%V_{\text{free:exs}}$. The points mark total $\%V_{\text{free}}$ at the experimental T_g for each of the 51 polymers in the sample set. The red curve shows an example of a melt curve, $\%V_{\text{free}}(T)$, the total percent free volume as a function of T for the case of the PS melt; the point where the $\%V_{\text{free}}(T)$ curve intersects the boundary is a prediction for (and is close

to) where PS becomes glassy. The plus sign is an independent evaluation of $\%V_{\text{free:vib}}$ at $T = T_g$ for the case of PS (see Figure 4) and it shows good agreement with the location of the proposed average $\%V_{\text{free:vib}}$ line.

Whether the proposed $\%V_{\text{free:vib}}$ plot is reasonably located can be tested using results for the one system (PS) for which we implemented a consistent data fit to both the melt and the glass. As noted, the apparent frozen-in excess free volume, $\%V_{\text{free:exs}}$, at T_g is 4.2%. The additional percent free volume must be all $\%V_{\text{free:vib}}$, which means that $\%V_{\text{free:vib}}$ is 4.2% below our total model $\%V_{\text{free}}$ value for PS at its T_g . We have marked this value for $\%V_{\text{free:vib}}$ with a "plus sign" in the figure. It falls a bit below, but still close to, the proposed average $\%V_{\text{vib:free}}$ line - and well within range considering the expected variation in slope ($\approx +/ - 0.7 \times 10^{-4} \text{ K}^{-1}$). With an estimate for $\%V_{\text{free:vib}}$ in place we have a well-defined route for estimating the excess value, $\%V_{\text{free:exs}}$, as the difference between $\%V_{\text{free}}$ and the average $\%V_{\text{free:vib}}$ line. Making use of the LCL prediction for the total $\%V_{\text{free}}$ for the PS melt as a function of temperature (the red curve in Figure 5) we are thus able to mark all of the free volume contributions ($\%V_{\text{free}}$, $\%V_{\text{free:exs}}$, and $\%V_{\text{free:vib}}$) directly on the figure.

This leads to the question: What does our black boundary line represent? Recall the boundary is a best fit line to predictions over our complete set of polymers for $\%V_{\text{free}}$, the total percent free volume, as the curve for each polymer is extrapolated down in temperature to its experimental glass transition. The boundary lies close to, but still just above the dashed blue line that estimates the average $\%V_{\text{free:vib}}$, the free volume associated with vibrational motions (gray area in the neighboring schematic). Recalling our discussion in section 3.4 centered around Figure 4, we expect that the free volume contained within a glassy sample will comprise both a vibrational contribution and a contribution associated with imperfect packing. This is in fact our interpretation of the black boundary line: All that is left in a melt's total free volume upon reaching T_g comes from the T -dependent vibrational contribution (which we view as an average) plus a small amount of excess from imperfect packing, and this combined total is apparently not enough for the system to remain as an equilibrium liquid.

In the spirit of Adam and Gibbs theory, one might consider the interpretation to be that, at some lowered level of $\%V_{\text{free:exs}}$, the number of cooperating segments needed to bring together *sufficient* excess free volume to cause the kinds of local rearrangements that are characteristic of a system in the melt state would be too large, and so the melt cannot persist. We will pursue this line of thought in the following section, in the context of contributions to the configurational entropy.

Continuing with the interpretation outlined above, note how in Figure 5 $\%V_{\text{free:exs}}$ at a given T_g would be given by the distance separating the solid black $\%V_{\text{free}}$ boundary line and the dashed blue line drawn for $\%V_{\text{vib:free}}$ at that temperature. Our results suggest that $\%V_{\text{free:exs}}$ at T_g , increases as the T_g of interest gets higher, although what we show in Figure 5 is not intended to be a quantitative prediction; it is also predicated on using an *average* α_G as a means of estimating a reasonable average T -dependence of $\%V_{\text{vib:free}}$ (and for simplicity, any curvature (likely positive) has been neglected). We would, however, wish to emphasize our conclusion that there is no evidence to support a single universal value for $\%V_{\text{free:exs}}$ at T_g , in contrast to the work of others, e.g. Simha and Boyer,²⁵ and Williams, Landel, and Ferry.¹⁹ Here we comment on what appears in Figure 5 to be a very low temperature intersection of the vibrational free volume ($\%V_{\text{free:vib}}$) and the $\%V_{\text{free}}$ at T_g correlation lines. We expect that more accurate "exact" curves would just gradually converge as T goes to zero, and not cross at some low finite T . The apparent crossing is just an artifact of expressing the average $\%V_{\text{free:vib}}$, and the $\%V_{\text{free}}$ at T_g correlation, both as simple lines.

In this section we have described a possible route for breaking down the two contributions $V_{\text{free:exs}}$ and $V_{\text{free:vib}}$ to the overall free volume, V_{free} . We have aimed at this goal because the two contributions to free volume are physically insightful, but difficult to separate out and quantify. However, as noted above, the Simha and Somcynski (SS) model equation of state actually does incorporate these two contributions *in principle*. The volume of the occupied "cells" in the model can

change with T and P and this represents the solid-like contribution (V_{vib}); there is also inclusion of unoccupied cells (holes), the number of which also changes with T, P , and this represents the excess free volume $V_{\text{free:exs}}$. However, if the intention of V_{vib} is to represent solid-like behavior (as in the Fox and Flory picture), the division in the SS model does not lead to a realistic prediction of contributions. In refs 40-42 for example, a number of polymers were characterized with the SS equation. Analysis of V_{vib} (called V_{occ} in those refs) showed that, on the one hand, it was compressible (changing with P) to a significant degree. On the other hand, this contribution exhibited thermal expansion that was an order of magnitude smaller than that of a typical polymeric solid/glass (see Table 1 and Figs. 3 and 4 in ref 40). For polymers, thermal expansion (α) for the solid or glass is commonly about a third of the value for the liquid (as can be seen by the blue dashed line in figure 5). The thermal expansion of V_{vib} (V_{occ}) from the SS equation is too weak to realistically represent solid-like behavior. Meanwhile, the thermal expansion of the hole fraction at constant pressure (meant to be the excess free volume) is therefore more analogous to the expansion of the *total* free volume. Related to this in ref 44, the hole fraction (" $\%V_{\text{free:exs}}$ ") at T_g was estimated for the same PS sample data we have analyzed and there it was found to be 7.63% which is almost double the value we estimate (4.2%); this would be necessary in the SS description in order to compensate for its failure to account for free volume contributions from the underlying solid.

3.7 Making Connections with the Entropy

As the glass transition is approached, the liquid $\%V_{\text{free}}$ curve for a given polymer approaches its solid $\%V_{\text{free:vib}}$ curve. This suggests a potential connection to concepts such as the "Kauzmann temperature", T_K , and the (closely-related) "ideal glass transition". (refs 3, 78, and 79 are examples of recent reviews covering these and related topics on glassy behavior.) At T_K , the difference in entropy between the supercooled liquid and the solid (formally the crystalline solid) is projected to disappear. As pointed out by Kauzmann,⁸⁰ this intersection (at $T > 0$) of liquid and

solid entropies upon decrease in T is anticipated due to the greater heat capacity of the liquid, analogous to the steeper slope of $V_l(T)$, related to $V_s(T)$. The evidently vanishing distinction between liquid and solid entropies plays an important role (through the configurational entropy) in the theories of Adam and Gibbs,¹² and Gibbs and Dimarzio.⁸¹ All of this, combined with the historically close connection between entropy and system volume, lead us to take a closer look at the LCL model entropy.

A link between entropy and *dynamics* in glass forming systems was made in the influential theory of Adam and Gibbs.¹² A key input in the theory is the "configurational entropy", S_c , and this is usually taken in practice to be the "excess entropy" (S_{excess}) defined by the entropy *difference* between liquid and solid. S_c can be thought of as a measure of the number of local potential energy minima ("stable configurations") available to a system,⁷⁹ and this can be largely reflected in the excess entropy. (However, details in vibrational characteristics of liquids and solids mean there are still distinctions between S_c and S_{excess} that deserve consideration.^{3,6,82}) The amount of configurational entropy available for a given T, P , determines the number, z^* , of nearby segments required to form a cooperatively rearranging group. That is, z^* is the minimum number of segments that together, add up to the critical amount of configurational entropy, s_c^* , needed to make a rearrangement. The Adam and Gibbs expression for the relaxation time, τ , is given by

$$\tau = A \exp[z^* \Delta \mu / k_B T] = A \exp[\Delta \mu s_c^* / k_B T S_c] \quad [16]$$

Here $\Delta \mu$ can be interpreted as a per-particle free energy of activation, where $z^* \Delta \mu$ is the Gibbs free energy difference between a z^* sized group that is (energetically) capable of rearranging, relative to that of the average z^* sized group.⁸³ Adam and Gibbs reasoned $\Delta \mu$ to be approximately a T -independent quantity, being determined mostly by the nature of the potential energy landscape. It is seen from eq 16 that $z^* = s_c^* / S_c$. That is, z^* is the critical amount of configurational entropy for a rearrangement (s_c^*), divided by the T, P dependent system configurational entropy

per segment (S_c , in per segment units, or other units consistent with s_c^*). As the configurational entropy decreases with decreasing T , the minimal number of segments (z^*) required for cooperative rearrangement increases, and this strongly drives up the relaxation times.

In testing the theory, Adam and Gibbs considered the ratio of relaxation times, in the form of $\ln[\tau/\tau_{\text{ref}}]$, and expressed them in terms of changes in configurational entropy ($S_c(T)$) determined by integrating the heat capacity differences between liquid and solid (glass). They were able to show that the theory gave close to the WLF functional form. Furthermore, the integrated expressions for configurational entropy were expressed in terms of the Kauzmann temperature (T_K) where $S_c(T_K) = 0.84$. From this, they were able to establish a formal connection between T_g and T_K (and thus entropy) by analyzing the T_K values implied from the experimental dynamics. The ratio T_g/T_K was found to be fairly reproducible, having a value of approximately 1.3 for a number of systems (with an average, $T_g - T_K$, of about 55 K), similar to what is typically observed when T_g and T_K are evaluated independently.

The work of Adam and Gibbs therefore provides a theoretical framework that shows how the approach to T_g is strongly correlated with the disappearance in the difference between the liquid and solid entropies. As we show below, our results for the LCL model entropy are consistent with this point of view. Before discussing this further we need to make an additional key connection between (the LCL) entropy and free volume.

The LCL model predicts a full range of thermodynamic properties. Note that the theoretical identification of what constitutes a ‘segment’ results from characterizing experimental data for a sample, as that yields values for r , the number of theoretical segments per chain, and v , the volume per segment. One consequence of this is that a model segment is not a chemical repeat unit, but rather

a theoretical measure of the relevant number of (externally coupled) degrees of freedom that contribute to a particular system's characteristic behavior. Figure 6 summarizes results for three measures of the entropy ($S = -\partial(A(N,V,T)/\partial T)_V$), calculated for the entire set of 51 polymer melts at their respective experimental T_g values, plotted against T_g . Parts (a), (b), and (c) summarize the results for, respectively, the entropy per mass, the entropy per volume, and the entropy per theoretical polymer segment.

The entropy per gram in the melt at $T = T_g$ (Fig. 6a) and the entropy per volume at $T = T_g$ (Fig. 6b) both show patterns that indicate some connection to the value of the polymer experimental T_g . However the strongest correlation by far is seen in the plot for the entropy per segment at T_g (Fig. 6c) vs. T_g , which exhibits a striking similarity to the pattern in the $\%V_{\text{free}}$ at T_g vs. T_g shown in Figure 3. This suggests a direct connection between the LCL entropy per theoretical segment and the LCL $\%V_{\text{free}}$, and that is confirmed by the results shown in the upper panel of Figure 7. In this plot the LCL model entropy per segment of all 51 polymer melts in the sample set, at the respective $T = T_g$, is plotted against the corresponding values of $\%V_{\text{free}}$ at $T = T_g$. The result is a smooth pattern, showing that the LCL entropy per segment is directly correlated with the theory's predictions of $\%V_{\text{free}}$ values. The trend in these reduced properties, *which does not depend on the molecular parameters*, is also evident for any single polymer melt in a plot of its entropy per segment (as it varies with T), against its $\%V_{\text{free}}$ (as it varies with T).

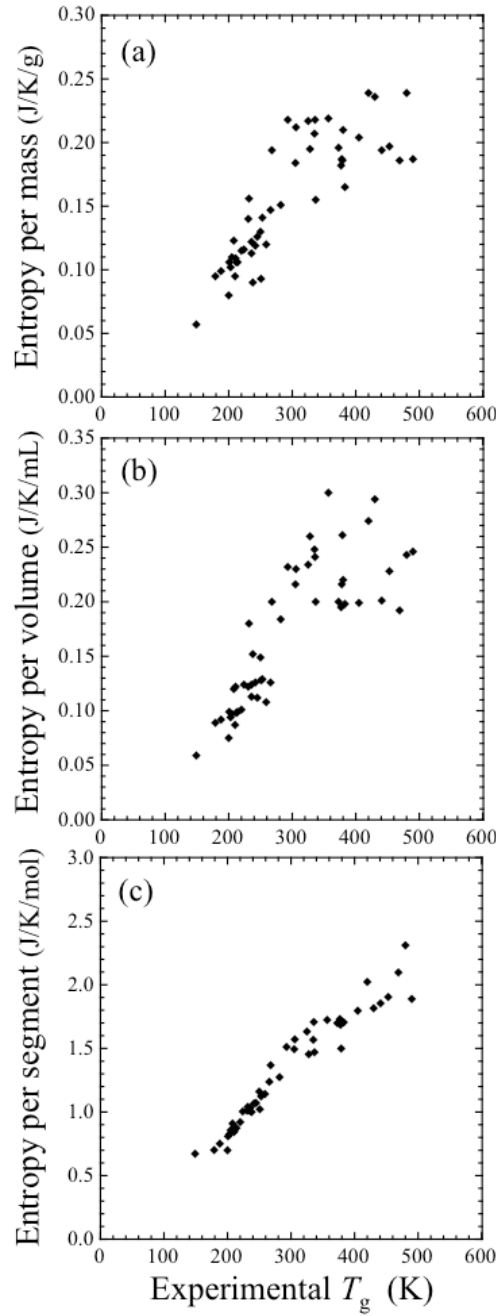


Figure 6. LCL model entropy of polymer melts at the experimental T_g plotted against the experimental T_g . Three quantifications of entropy are considered. The upper panel shows entropy per gram (units of $(J/K)/g$). The middle panel shows entropy per volume (units of $(J/K)/mL$). The lower panel shows entropy per LCL theoretical segment, which is the total model entropy divided by the total number of segments, Nr (the number of molecules multiplied by the number of segments per molecule), units of J/K .

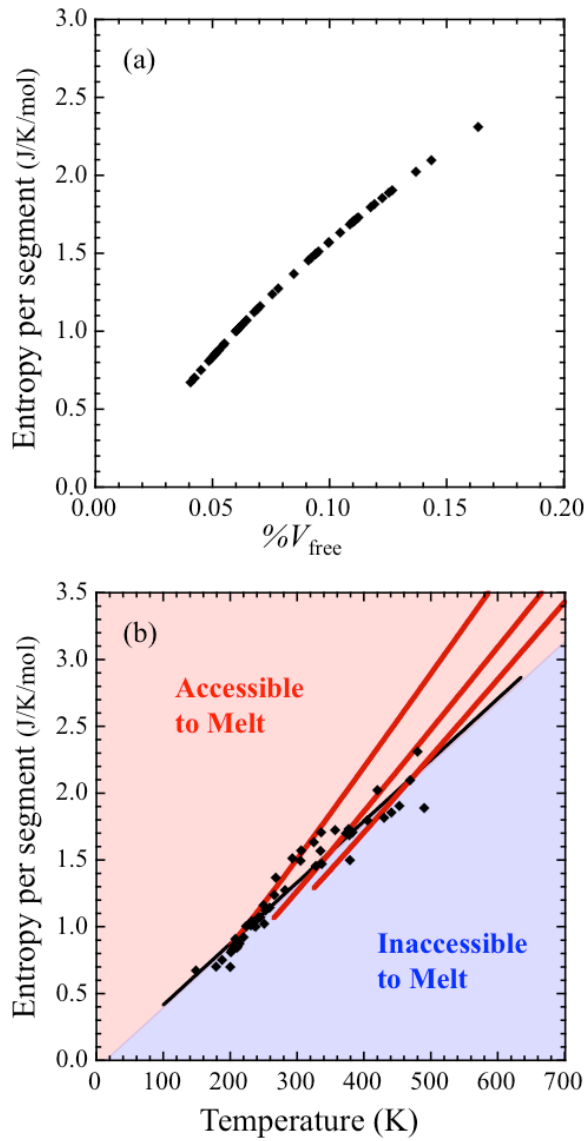


Figure 7. Relating the LCL model entropy per segment to $\%V_{\text{free}}$, and thus to a boundary of minimum entropy per segment. The upper panel shows the LCL model entropy per segment of all 51 polymer melts in the sample set at the respective $T = T_g$ plotted against the corresponding values of $\%V_{\text{free}}$ at $T = T_g$. The pattern shows the connection of two reduced properties of the model thus the same the pattern is traced out by any single polymer (regardlesss of its molecular parameters) in a plot of its entropy per segment as a function of T . The lower panel shows how the entropy per segment at T_g vs. T_g functions as a T -dependent boundary of minimum entropy per segment. The best fit boundary line is the heavy black line below which is inaccessible to the melt. Also shown is the track of an example melt curve (for PS) which is steeper than the boundary, and upon the intersection of the melt curve with the boundary the system is predicted to go glassy. The temperature dependence of the entropy per segment boundary is an indication that T_g occurs when the melt entropy has decreased to the point that is nearing the value of the corresponding solid.

The connection between entropy per segment and $\%V_{\text{free}}$ leads to the notion that plotting the entropy per segment at T_g vs. T_g would create a boundary similar to that (Fig. 6c) of minimum melt $\%V_{\text{free}}$, discussed above, and this is exactly what is shown in Fig. 7b. In that plot a boundary line is drawn, and shading added, to mark the regions that are accessible and inaccessible to the melt. Also shown as examples are the tracks of three melt curves as a function of temperature (the same melts as in Figure 3, PBA, PS, and TMPC): As T decreases, a melt curve, which is steeper than the boundary, drops to a point where it intersects the boundary. The intersection of the melt curve with the boundary is the predicted value for the T_g of that polymer. Note that this would not have been as clear had we used one of the other measures of entropy (i.e. per gram or per mL).

By arguments analogous to those used above in relating the T -dependent approach of $\%V_{\text{free}}$ to the underlying $\%V_{\text{free:vib}}$, we interpret our results as illustrating how the difference between the liquid and solid entropies diminishes as the melt approaches the glassy state, as has often been discussed^{3,78,79} in describing the approach to the Kauzmann temperature, as well as in the theory of Adam and Gibbs.¹²

3.8 Free Volume Is Just One Variable, Temperature Is the Other

Throughout this article our model predictions have focused on results at atmospheric pressure only, and it was under these conditions that the historical free volume models gained their traction. Over the years free volume models have come into question, however, and one reason is that they have been found to fail in explaining data from pressure-dependent measurements.¹⁻⁹ Detailed comments on one particular free volume model⁸⁵ that had aimed to account for P -dependence are below. A general problem in assuming that free volume is the *only* variable to explain the dynamics is, if one changes the T and P in such a way that the system volume remains *fixed* then the dynamics would not be expected to change; but, they do.^{1,8,86-88} An increase in T , with V fixed, contributes to increased dynamics through increased available energy for activated processes. Thus it is important to

emphasize that even a model that shows free volume to play an important role, such as the LCL theory, should sensibly reflect multiple influences on dynamic behavior.

Consider how the relaxation time, or viscosity, will change as the volume (and thus free volume) is varied using two possible experimental paths: along an isotherm versus along an isobar. Typically, the relaxation times will decrease more steeply with increasing V for the cases where V varies along an isobar; the drop is not as steep when V increases along an isotherm. (A nice example of this is shown in Figures 10 and 11 of Roland et al.¹ for relaxation times of poly(methyltolylsiloxane); also clear, are the differing τ values where these isobars and isotherms reach any single chosen V , which demonstrates the change in τ with T at constant V . In the case where volume increases along an isobar the strong increase in dynamics is promoted by both the increases in free volume and in temperature. Note that the effect of temperature goes beyond just the simple fact that V increases with T at constant P , if this were the only consideration then the results for change in V along the isotherm would be the same as any other path traversing the same V values.

There have been attempts to model the T,P -dependence of dynamics while maintaining a solely free volume-based point of view, e.g. the model described in Ferry.⁸⁵ Note that while there is no way for *total* $\%V_{\text{free}}$ (as defined in this work) to change if the total system volume is fixed, it is possible (though we are not advocating this point of view) to propose that there are significant *excess* free volume changes that can occur when V , and the total V_{free} are fixed. It would then be logical to consider two independent variables upon which the $V_{\text{free:exs}}$ depends, e.g T,P , or T,V , etc.. The model in ref 85 is thus based on the hypothesis that the dynamics can be controlled *solely* by changes in $V_{\text{free:exs}}$, which thus varies as a function of T,P . This model can be analyzed by considering how T and P vary along an isochoric path (the total system volume is fixed) compared to an "isochronic" path, where T and P change so as to produce no net change in dynamics (constant τ).

The former condition is given by $(\partial P / \partial T)_V = \alpha_L / \kappa_L$, while the latter, if one assumes $V_{\text{free:exs}}$ solely controls dynamics, is given by $(\partial P / \partial T)_\tau = \alpha_{\text{exs}} / \kappa_{\text{exs}} = (\alpha_L - \alpha_{\text{vib}}) / (\kappa_L - \kappa_{\text{vib}})$. (Additional details are provided in the appendix.) Experimentally it is found that $(\partial P / \partial T)_\tau$ is significantly larger than $(\partial P / \partial T)_V$; for example, $(\partial P / \partial T)_\tau = 4$ to 6 MPa/K for polymers in ref 85, Table 11-III. The assumption that dynamics are controlled by $V_{\text{free:exs}}$ therefore implies that $\alpha_{\text{exs}} / \kappa_{\text{exs}}$ must be significantly larger than α_L / κ_L , or, equivalently, the vibrational free volume (the "occupied volume") must be significantly more compressible than the excess free volume. This conceptually difficult implication has been noted about the model.^{1,4}

In fact, we have checked the proposal that $\alpha_{\text{exs}} / \kappa_{\text{exs}} \approx (\partial P / \partial T)_\tau$ via an estimate of $\alpha_{\text{exs}} / \kappa_{\text{exs}}$ using experimental values⁸⁹ for liquid and crystal α 's and κ 's to stand for $[\alpha_L, \kappa_L, \alpha_{\text{vib}}, \kappa_{\text{vib}}]$ for the case of OTP (details in appendix). The result is $\alpha_{\text{exs}} / \kappa_{\text{exs}} \approx 1.35$ MPa/K, whereas the experimental value for $(\partial P / \partial T)_\tau \approx 3.7$ MPa/K.⁹⁰ In fact, $\alpha_{\text{exs}} / \kappa_{\text{exs}}$ is actually much closer to the overall $(\partial P / \partial T)_V = \alpha_L / \kappa_L = 1.22$ MPa/K. Similar conclusions follow for polymers using glassy data for α_{vib} and κ_{vib} (also covered in the appendix). The condition of constant excess free volume *does not* correspond well to the condition of constant relaxation time, and thus, $\%V_{\text{free:exs}}$, at least according to the definitions given here, does not appear to vary in such a way that it could explain the dynamics, as a single quantity by itself.

We conclude that a robust point of view should consider the dynamic response to be determined by the combined contributions of both temperature *and* volume. In this we concur with the insight provided from pressure dependent studies (examples reviewed in ref 1). An interesting form of analysis has been done by Casalini, Roland, and coworkers^{88,91} where they explore a general relation showing $\ln \tau \propto 1/(TV^\gamma)$ (or $\ln \tau \propto \rho^\gamma / T$), where γ is a species-specific parameter. Another example is the form, $(\rho - \rho^*)/T$, where ρ^* is a species-specific parameter;⁹²

additional scaling-type analyses have been discussed in ref 93.) The $\ln \tau \propto 1/(TV^\gamma)$ scaling means that over P -dependent data, the value of the single combined variable, TV^γ , is what uniquely determines the relaxation time; different combinations of the separate values of T and V can lead to the same τ , and thus to collapse of the data onto a single curve dependent on TV^γ , alone. The values of γ can be compared for different species and provides a measure of temperature- vs. volume-sensitivity for a given system (see for example Table 1 in ref 2). We expect that some of these ideas for free volume analysis will be useful as we continue with our own studies, for example, in our analysis of dynamics over a broad PVT space.

We believe another effective route to showing how the effects of (free) volume and temperature combine is through the Adam and Gibbs theory. Unlike the traditional free volume models, the AG theory has been able to account for the more general scenario where pressure can be variable.⁹⁴⁻⁹⁶ (See note.⁹⁷) Note that both T and S_c contribute explicitly through the product TS_c within the AG expression, $\tau = A \exp[\Delta \mu s_c^*/k_B T S_c]$ (eq 16). This allows for dynamics to increase with increased temperature, even if the entropy and free volume remain roughly fixed (the traditional free volume models don't have this ability). The connection we have made in this work between free volume and entropy, now envisioned within the context of the theory of Adam and Gibbs, thus provides some grounding for how free volume plays its role in glass forming liquids, where the implication is that it should appear in a more explicit combination with temperature. Unlike the traditional free volume models, this should allow for how either an increase in temperature *or* an increase in free volume (or both) will be able to increase the dynamics. We intend to explore these ideas in future work covering more general pressure dependent scenarios.

Summary and Conclusions

The concept of 'free volume' and its connection to the polymeric glass transition has had a somewhat muddled history. The fact that both the former and the latter, themselves, lack the definitive clarity of unambiguous properties such as, e.g. total volume, and a (crystalline) melting temperature, has resulted in a literature that is confusing to follow and distinctly nonlinear, in the sense that later efforts have not always represented clear progress relative to earlier ones.

This Perspective began with a summary of the key concepts and how they are related. In particular, we explicitly described the issues that arise from the fact that different models use different definitions of what constitutes free volume. As an example, both the *total* free volume (V_{free}) and *excess* free volume ($V_{\text{free:exs}}$) have been denoted simply as "free volume" in past works. A goal in surveying the various definitions of free volume, e.g. those from Fox and Flory, Simha and Boyer, Cohen and Turnbull, Doolittle, and WLF, etc., was to place them into a context that is tethered to a physical picture of what each contribution represents. We also discussed the implications when alternative estimates for free volume are inserted into relationships that aim to connect it with experimentally measurable properties, such as relaxation times and viscosity. A related issue involves the difference in characterizing free volume using dynamics measurements, versus equation of state (i.e. volumetric) data.

With that context firmly in mind, we turned to our own, new, efforts in applying the Locally Correlated Lattice (LCL) model to define polymeric free volume. We showed for a set of over fifty polymers that our predictions of percent free volume (at the respective glass transition temperatures) increases in a linear fashion with the experimentally-measured glass transition temperature, leading us to propose that there is a temperature-dependent amount of 'minimum percent free volume' that a polymer must be able to access in order to maintain a melt state. Going further, we interpret this minimum as an upper bound on the free

volume associated with a corresponding solid-like state. That is, the boundary of minimum $\%V_{\text{free}}$ is comprised by contributions from simple vibrational motions ($\%V_{\text{free:vib}}$), plus, a small amount associated with packing imperfections. In this view we find ourselves in agreement with the picture described decades ago by Fox and Flory. Conversely, our calculations do not support the notion that the excess free volume at the glass transition is a single universal constant; via two forms of analysis, we predict values that are small (several percent), but likely vary from polymer to polymer; it may be possible to say more about this in the future if more glassy samples can be analyzed, especially for low- T_g polymers.

Because the LCL theory is a first-principles thermodynamic description we are also able to make a fundamental connection between percent free volume and entropy per theoretical segment. We thus have found (analogous to $\%V_{\text{free}}$) a T -dependent boundary of minimum entropy per segment obeyed over our set of polymers at their respective $T = T_g$. This leads us to connect our observation of decreasing excess free volume to the vanishing difference between the entropies of the melt and solid states (the excess entropy). The result is a clear link to the work of Adam and Gibbs, and thus to the dramatic increase in relaxation times and viscosity as T drops to near the glass transition.

Finally, we turned to a key result that we wish to highlight: Our LCL results point to the linked importance of free volume and temperature in controlling how melt properties change as the glass transition is approached. Experimental evidence is clear that following an isochoric, rather than the usual isobaric, path to the glass transition still leads to substantial temperature-dependent changes in dynamic properties. Sensible free volume analyses must account for this fact. In addition, we note the explicit dependence on both, temperature and entropy (and thus, temperature and free volume) in the Adam and Gibbs expression. We expect that using our thermodynamic approach, through the LCL model, will lead to greater clarity in how to assess the role that free volume plays and how that role is balanced with temperature, and this will be the goal of future studies.

Acknowledgment

We gratefully acknowledge the financial support provided by the National Science Foundation (DMR-1403757).

References and Notes

- (1) Roland, C.; Hensel-Bielowka, S.; Paluch, M.; Casalini, R. Supercooled dynamics of glass-forming liquids and polymers under hydrostatic pressure. *Reports on Progress in Physics* **2005**, *68*, 1405-1478.
- (2) Roland, C. M. Relaxation Phenomena in Vitrifying Polymers and Molecular Liquids. *Macromolecules* **2010**, *43*, 7875-7890.
- (3) Cangialosi, D. Dynamics and thermodynamics of polymer glasses. *Journal of Physics-Condensed Matter* **2014**, *26*, 153101.
- (4) Floudas, G. *Broadband Dielectric Spectroscopy*, chapter 8, eds. Kremer, F. and Schonhals, A.; Springer: Berlin, 2003.
- (5) Debenedetti, P.G. *Metastable Liquids*; Princeton University Press: Princeton, 1996.
- (6) Angell, C.A.; Borick, S. Specific heats C-p, C-v, C-conf and energy landscapes of glassforming liquids. *J. Non Cryst. Solids* **2002**, *307*, 393-406.
- (7) Goldstein, M. Viscous Liquids and the Glass Transition. IV. Thermodynamic Equations and the Transition *J. Phys. Chem.* **1973**, *77*, 667-673.
- (8) Ferrer, M.; Lawrence, C.; Demirjian, B.; Kivelson, D.; Alba-Simionescu, C.; Tarjus, G. Supercooled liquids and the glass transition: Temperature as the control variable. *J. Chem. Phys.* **1998**, *109*, 8010-8015.
- (9) Corezzi, S.; Capaccioli, S.; Casalini, R.; Fioretto, D.; Paluch, M.; Rolla, P. Check of the temperature- and pressure-dependent Cohen-Grest equation. *Chemical Physics Letters* **2000**, *320*, 113-117.
- (10) White, R. P.; Lipson, J. E. G. Free Volume in the Melt and How It Correlates with Experimental Glass Transition Temperatures: Results for a Large Set of Polymers. *Acs Macro Letters* **2015**, *4*, 588-592.
- (11) White, R. P.; Lipson, J. E. G. Free Volume, Cohesive Energy Density, and Internal Pressure as Predictors of Polymer Miscibility. *Macromolecules* **2014**, *47*, 3959-3968.
- (12) Adam, G.; Gibbs, J. H. On Temperature Dependence of Cooperative Relaxation Properties in Glass-Forming Liquids. *J. Chem. Phys.* **1965**, *43*, 139-146.
- (13) Andrade, E. N. D. C. The viscosity of liquids. *Nature* **1930**, *125*, 309-310.

(14) Doolittle, A. K. Studies in Newtonian Flow .2. the Dependence of the Viscosity of Liquids on Free-Space. *J. Appl. Phys.* **1951**, *22*, 1471-1475.

(15) We have plotted all of Doolittle's data (Table II, ref 14). For six out of the nine alkanes (sets with > 2 data points), fits to an Arrhenius form are better than the Doolittle form (in terms of correlation coefficient, R^2 , or Doolittle's measure of sum percent error), though in all cases differences are not large. Doolittle did not provide results for any fits other than n-heptadecane, and in that case, two lower T points were disregarded which if anything, might not seem sensible given that departure from Arrhenius behavior is expected at lower T . Results can be provided upon request.

(16) Vogel, H. The temperature dependence law of the viscosity of fluids. *Physikalische Zeitschrift* **1921**, *22*, 645-646.

(17) Fulcher, G. S. Analysis of recent measurements of the viscosity of glasses. *J Am Ceram Soc* **1925**, *8*, 339-355.

(18) Tammann, G.; Hesse, W. The dependancy of viscosity on temperature in hypothermic liquids. *Zeitschrift Fur Anorganische Und Allgemeine Chemie* **1926**, *156*.

(19) Williams, M. L.; Landel, R. F.; Ferry, J. D. Mechanical Properties of Substances of High Molecular Weight .19. the Temperature Dependence of Relaxation Mechanisms in Amorphous Polymers and Other Glass-Forming Liquids. *J. Am. Chem. Soc.* **1955**, *77*, 3701-3707.

(20) Fox, T. G.; Flory, P. J. 2nd-Order Transition Temperatures and Related Properties of Polystyrene .1. Influence of Molecular Weight. *J. Appl. Phys.* **1950**, *21*, 581-591.

(21) Fox, T. G.; Flory, P. J. Further Studies on the Melt Viscosity of Polyisobutylene. *Journal of Physical and Colloid Chemistry* **1951**, *55*, 221-234.

(22) Fox, T. G.; Flory, P. J. The Glass Temperature and Related Properties of Polystyrene - Influence of Molecular Weight. *Journal of Polymer Science* **1954**, *14*, 315-319.

(23) Aharoni, S. M. Thermal Dilatation of Polymers. *Journal of Macromolecular Science-Physics* **1974**, *B 9*, 699-731.

(24) Cohen, M. H.; Turnbull, D. Molecular Transport in Liquids and Glasses. *J. Chem. Phys.* **1959**, *31*, 1164-1169.

(25) Simha, R.; Boyer, R. F. On a General Relation Involving Glass Temperature and Coefficients of Expansion of Polymers. *J. Chem. Phys.* **1962**, *37*, 1003-1007.

(26) Cohen, M. H.; Grest, G. S. Liquid-Glass Transition, a Free-Volume Approach. *Physical Review B* **1979**, *20*, 1077-1098.

(27) Paluch, M.; Casalini, R.; Roland, C. M. Cohen-Grest model for the dynamics of supercooled liquids. *Physical Review E* **2003**, *67*, 021508.

(28) Angell, C.A., in *Relaxations of Complex Systems*, eds. Ngai, K.L. and Wright, G.B.; National Technical Information Service, U.S. Department of Commerce, Springfield, VA, 1985.

(29) Angell, C.A. Formation of Glasses from Liquids and Biopolymers. *Science* **1995**, *267*, 1924-1935.

(30) Rodgers, P. A. Pressure Volume Temperature Relationships for Polymeric Liquids - a Review of Equations of State and their Characteristic Parameters for 56 Polymers. *J. Appl. Polym. Sci.* **1993**, *48*, 1061-1080.

(31) Berthier, L.; Biroli, G. Theoretical Perspective in the Glass Transition and Amorphous Materials. *Rev. Mod. Phys.* **2011**, *83*, 587-645.

(32) Dyre, J.C. The Glass Transition and Elastic Models of Glass-Forming Liquids. *Rev. Mod. Phys.* **2006**, *78*, 953-972.

(33) Dudowicz, J.; Freed, K. F.; Douglas, J. F. Entropy theory of polymer glass formation revisited. I. General formulation. *J. Chem. Phys.* **2006**, *124*, 064901.

(34) Dudowicz, J.; Freed, K. F.; Douglas, J. F. Generalized Entropy Theory of Polymer Glass Formation. *Advances in Chemical Physics*, Vol 137 **2008**, *137*, 125-222.

(35) Xu, W.; Freed, K. F. Influence of Cohesive Energy and Chain Stiffness on Polymer Glass Formation. *Macromolecules* **2014**, *47*, 6990-6997.

(36) Dudowicz, J.; Freed, K. F.; Madden, W. G. Role of Molecular-Structure on the Thermodynamic Properties of Melts, Blends, and Concentrated Polymer-Solutions - Comparison of Monte-Carlo Simulations with the Cluster Theory for the Lattice Model. *Macromolecules* **1990**, *23*, 4803-4819.

(37) Freed, K. F.; Dudowicz, J. Influence of monomer molecular structure on the miscibility of polymer blends. *Phase Behavior of Polymer Blends* **2005**, *183*, 63-126.

(38) Simha, R.; Somcynsk.T On Statistical Thermodynamics of Spherical and Chain Molecule Fluids. *Macromolecules* **1969**, *2*, 342-350.

(39) Simha, R. Configurational Thermodynamics of Liquid and Glassy Polymeric States. *Macromolecules* **1977**, *10*, 1025-1030.

(40) Dlubek, G.; Sen Gupta, A.; Pionteck, J.; Krause-Rehberg, R.; Kaspar, H.; Lochhaas, K. Temperature dependence of the free volume in fluoroelastomers from positron lifetime and PVT experiments. *Macromolecules* **2004**, *37*, 6606-6618.

(41) Dlubek, G.; Wawryszczuk, J.; Pionteck, J.; Goworek, T.; Kaspar, H.; Lochhaas, K. High-pressure dependence of the free volume in fluoroelastomers from positron lifetime and PVT experiments. *Macromolecules* **2005**, *38*, 429-437.

(42) Kilburn, D.; Dlubek, G.; Pionteck, J.; Alam, M. A. Free volume in poly(n-alkyl methacrylate)s from positron lifetime and PVT experiments and its relation to the structural relaxation. *Polymer* **2006**, *47*, 7774-7785.

(43) Dlubek, G.; Kilburn, D.; Alam, M. Comments to the paper "The need to reconsider traditional free volume theory for polymer electrolytes". *Electrochim. Acta* **2004**, *49*, 5241-5247.

(44) Utracki, L. A. Pressure-volume-temperature of molten and glassy polymers. *Journal of Polymer Science Part B-Polymer Physics* **2007**, *45*, 270-285.

(45) Utracki, L. A.; Sedlacek, T. Free volume dependence of polymer viscosity. *Rheologica Acta* **2007**, *46*, 479-494.

(46) Utracki, L.; Simha, R. Free volume and viscosity of polymer-compressed gas mixtures during extrusion foaming. *Journal of Polymer Science Part B-Polymer Physics* **2001**, *39*, 342-362.

(47) Sorrentino, A.; Pantani, R. Pressure-dependent viscosity and free volume of atactic and syndiotactic polystyrene. *Rheologica Acta* **2009**, *48*, 467-478.

(48) Lipson, J. E. G.; White, R. P. Connecting Theory and Experiment To Understand Miscibility in Polymer and Small Molecule Mixtures. *J. Chem. Eng. Data* **2014**, *59*, 3289-3300..

(49) White, R. P.; Lipson, J. E. G. Chain fluids: Contrasts of theoretical and simulation approaches, and comparison with experimental alkane properties. *J. Chem. Phys.* **2009**, *131*, 074109.

(50) Luettmer-Strathmann, J.; Lipson, J. E. G. Miscibility of polyolefin blends. *Macromolecules* **1999**, *32*, 1093-1102.

(51) White, R. P.; Lipson, J. E. G.; Higgins, J. S. How Pure Components Control Polymer Blend Miscibility. *Macromolecules* **2012**, *45*, 8861-8871.

(52) DeFelice, J.; Lipson, J. E. G. Polymer Miscibility in Supercritical Carbon Dioxide: Free Volume as a Driving Force. *Macromolecules* **2014**, *47*, 5643-5654.

(53) Zoller, P.; Walsh, D. *Standard Pressure-Volume-Temperature Data for Polymers*; Technomic Pub Co.: Lancaster, PA, 1995.

(54) Callaghan, T. A.; Paul, D. R. Interaction Energies for Blends of Poly(methyl Methacrylate), Polystyrene, and Poly(alpha-Methylstyrene) by the Critical Molecular-Weight Method. *Macromolecules* **1993**, *26*, 2439-2450.

(55) Tabulated values for these data were made available to us by D.J. Lohse.

(56) Yi, Y.X.; Zoller, P. An Experimental and Theoretical-Study of the Pvt Equation of State of Butadiene and Isoprene Elastomers to 200-Degrees-C and 200-Mpa. *Journal of Polymer Science Part B-Polymer Physics* **1993**, *31*, 779-788.

(57) Olabisi, O.; Simha, R. Pressure-Volume-Temperature Studies of Amorphous and Crystallizable Polymers .1. Experimental. *Macromolecules* **1975**, *8*, 206-210.

(58) Kim, C.K.; Paul, D.R. Interaction Parameters for Blends Containing Polycarbonates .1. Tetramethyl Bisphenol-a Polycarbonate Polystyrene *Polymer* **1992**, *33*, 1630-1639.

(59) Ougizawa, T.; Dee, G. T.; Walsh, D. J. Pressure Volume Temperature Properties and Equations of State in Polymer Blends - Characteristic Parameters in Polystyrene Poly(vinyl Methyl-Ether) Mixtures. *Macromolecules* **1991**, *24*, 3834-3837.

(60) Mark, J.E. *Polymer Data Handbook*; Oxford University Press: Oxford, 1999.

(61) Aharoni, S.M. Molecular Stiffness and Thermal-Properties of Polymers. *J Appl Polym Sci* **1976**, *20*, 2863-2869.

(62) Davis, G.; Eby, R. Glass Transition of Polyethylene - Volume Relaxation. *J. Appl. Phys.* **1973**, *44*, 4274-4281.

(63) Han, S.; Gregg, C.; Radosz, M. How the solute polydispersity affects the cloud-point and coexistence pressures in propylene and ethylene solutions of alternating poly(ethylene-co-propylene). *Ind Eng Chem Res* **1997**, *36*, 5520-5525.

(64) Santangelo, P.; Ngai, K.; Roland, C. Temperature dependence of relaxation in polypropylene and poly(ethylene-co-propylene). *Macromolecules* **1996**, *29*, 3651-3653.

(65) Cowie, J. Glass Transition Temperatures of Stereoblock, Isotactic and Atactic Polypropylenes of various Chain Lengths. *European Polymer Journal* **1973**, *9*, 1041-1049.

(66) Hattam, P.; Gauntlett, S.; Mays, J. W.; Hadjichristidis, N.; Young, R. N.; Fetters, L. J. Conformational Characteristics of some Model Polydienes and Polyolefins. *Macromolecules* **1991**, *24*, 6199-6209.

(67) Liu, T.; Garner, P.; DeSimone, J. M.; Roberts, G. W.; Bothun, G. D. Particle formation in precipitation polymerization: Continuous precipitation polymerization of acrylic acid in supercritical carbon dioxide. *Macromolecules* **2006**, *39*, 6489-6494.

(68) Rindfleisch, F.; DiNoia, T. P.; McHugh, M. A. Solubility of polymers and copolymers in supercritical CO₂. *J. Phys. Chem.* **1996**, *100*, 15581-15587.

(69) Cowie, J. M. G.; McEwen, I. J. Molecular Motions in Poly(dimethyl Siloxane)oligomers and Polymers. *Polymer* **1973**, *14*, 423-426.

(70) Yu, J. Y.; Li, B. Z.; Lee, S. W.; Ree, M. H. Relationship between physical properties and chemical structures of poly(ethylene terephthalate-co-ethylene isophthalate). *J Appl Polym Sci* **1999**, *73*, 1191-1195.

(71) Liu, A.S.; Liau, W.B.; Chiu, W.Y. Studies on blends of binary crystalline polymers. 1. Miscibility and crystallization behavior in poly(butylene terephthalate) polyarylates based on bisphenol A isophthalate *Macromolecules* **1998**, *31*, 6593-6599.

(72) Engelberg, I.; Kohn, J. Physicomechanical Properties of Degradable Polymers used in Medical Applications - a Comparative-Study. *Biomaterials* **1991**, *12*, 292-304.

(73) Boyer, R. F.; Spencer, R. S. Thermal expansion and second-order transition effects in high polymers part I experimental results. *J. Appl. Phys.* **1944**, *15*, 398-405.

(74) Stickel, F.; Fischer, E. W.; Richert, R. Dynamics of glass-forming liquids .2. Detailed comparison of dielectric relaxation, dc-conductivity, and viscosity data. *J. Chem. Phys.* **1996**, *104*, 2043-2055.

(75) Schmidtke, B.; Hofmann, M.; Lichtinger, A.; Rossler, E.A. Temperature Dependence of the Segmental Relaxation Time of Polymers Revisited. *Macromolecules* **2015**, *48*, 3005-3013.

(76) Lewis, O. G. Relationships between Polymer Structure and Glass Temperature I. N-Alkanes. *J. Chem. Phys.* **1965**, *43*, 2693-2696.

(77) Miller, A.A. Kinetic Interpretation of the Glass Transition: Glass Temperatures of n-Alkane Liquids and Polyethylene *J. Polym. Sci. A-2* **1968**, *6*, 249-257.

(78) Stillinger, F. H.; Debenedetti, P. G. Glass Transition Thermodynamics and Kinetics. *Annual Review of Condensed Matter Physics, Vol 4* **2013**, *4*, 263-285.

(79) Debenedetti, P. G.; Stillinger, F. H. Supercooled liquids and the glass transition. *Nature* **2001**, *410*, 259-267.

(80) Kauzmann, W. The Nature of the Glassy State and the Behavior of Liquids at Low Temperatures. *Chem. Rev.* **1948**, *43*, 219-256.

(81) Gibbs, J. H.; Dimarzio, E. A. Nature of the Glass Transition and the Glassy State. *J. Chem. Phys.* **1958**, *28*, 373-383.

(82) Martinez, L.-M.; Angell, C.A. A Thermodynamic Connection to the Fragility of Glass-Forming Liquids. *Nature* **2001**, *410*, 663-667.

(83) Using a "[z,P,T] ensemble", Adam and Gibbs had first expressed the probability that a group of z segments, is capable of rearranging; this was given by $\exp[-(G'-G)/kT]$ where $G'-G$ is the Gibbs free energy difference between size z groups that are capable and incapable respectively. This probability was re-written as a function of the number of cooperating segments giving $\exp[-z\Delta\mu/k_B T]$ where $\Delta\mu$ is the per-segment Gibbs free energy difference (thus $z\Delta\mu = (G'-G)$).

(84) Technically, rather than T_K , Adam and Gibbs identified this as " T_2 " their Gibbs and Dimarzio ideal glass transition temperature (second order transition), where the configurational entropy is zero. Given their integration over the heat capacity differences of liquid and solid to define changes in configurational entropy, it is

reasonable just to call this the Kauzmann temperature, T_K , and thus avoid the debate of whether an actual thermodynamic transition occurs at T_K .

(85) Ferry, J.D. *Viscoelastic Properties of Polymers*, second edition; Wiley: New York, 1970.

(86) Floudas, G.; Mpoukouvalas, K.; Papadopoulos, P. The Role of Temperature and Density on the Glass-Transition Dynamics of Glass Formers. *J. Chem. Phys.* **2006**, *124*, 074905.

(87) Paluch, M.; Roland, C. M.; Casalini, R.; Meier, G.; Patkowski, A. The Relative Contributions of Temperature and Volume to Structural Relaxation of van der Waals Molecular Liquids. *J. Chem. Phys.* **2003**, *118*, 4578-4582.

(88) Casalini, R.; Mohanty, U.; Roland, C. M. Thermodynamic interpretation of the scaling of the dynamics of supercooled liquids. *J. Chem. Phys.* **2006**, *125*, 014505.

(89) Naoki, M.; Koeda, S. Pressure-Volume-Temperature Relations of Liquid, Crystal, and, Glass of *o*-Terphenyl. Excess Amorphous Entropies and Factors Determining Molecular Mobility. *J. Phys. Chem.* **1989**, *93*, 948-955.

(90) Naoki, M.; Endou, H.; Matsumoto, K. Pressure Effects on Dielectric Relaxation of Supercooled *o*-Terphenyl. *J. Phys. Chem.* **1987**, *91*, 4169-4174.

(91) Casalini, R.; Roland, C. M. Thermodynamical scaling of the glass transition dynamics. *Physical Review E* **2004**, *69*, 062501.

(92) Alba-Simionescu, C.; Cailliaux, A.; Alegria, A.; Tarjus, G. Scaling out the density dependence of the α relaxation in glass-forming polymers. *Europhys. Lett.* **2004**, *68*, 58-64.

(93) Ngai, K.L.; Habasaki, J.; Prevosto, D.; Capaccioli, S.; Paluch, M. Thermodynamic Scaling of the α -Relaxation Time and Viscosity Stems from the Johari-Goldstein β -Relaxation or the Primitive Relaxation of the Coupling Model. *J. Chem. Phys.* **2012**, *137*, 034511.

(94) Casalini, R.; Capaccioli, S.; Lucchesi, M.; Rolla, P.; Corezzi, S. Pressure dependence of structural relaxation time in terms of the Adam-Gibbs model. *Physical Review E* **2001**, *63*, 031207.

(95) Prevosto, D.; Capaccioli, S.; Lucchesi, M.; Leporini, D.; Rolla, P. Pressure and temperature dependence of structural relaxation dynamics in polymers: a thermodynamic interpretation. *Journal of Physics-Condensed Matter* **2004**, *16*, 6597-6608.

(96) Schwartz, G.; Tellechea, E.; Colmenero, J.; Alegria, A. Correlation between temperature-pressure dependence of the alpha-relaxation and configurational entropy for a glass-forming polymer. *J. Non Cryst. Solids* **2005**, *351*, 2616-2621.

(97) Here, changes in entropy with pressure are determined, and as noted above, the distinction between S_{excess} and S_c should be considered; it is believed S_{excess} and S_c can be roughly proportional to each other (e.g. refs 3, 6, 82) which helps in fitting the Adam and Gibbs form.

Appendix A: Background on LCL Model and Fitting

The derivation of the LCL model starts by considering a fluid of N chain-like molecules in a total volume, V , at absolute temperature, T . The chain molecule fluid is discretized on a lattice wherein the lattice sites can be occupied by a molecular segment, or unoccupied (vacant); the incorporation of vacant sites thus makes the model compressible. As noted in the main text, the three key molecular level parameters are: r , the number of segments per chain molecule, v , the volume per lattice site (same as the volume of a molecular segment), and ε , the non-bonded segment-segment interaction energy between near neighbor segments. An integral equation approach is applied in formulating approximate expressions for the near neighbor site-site probabilities; these are local correlations, e.g., the probability of whether a neighboring site next to a segment is vacant, or occupied by another segment. From these temperature-dependent probabilities the internal energy (U) can be computed (summed over all segments in the system), and then the Helmholtz free energy (A) is obtained via thermodynamic integration from an athermal reference state using the Gibbs-Helmholtz relationship ($\partial(A/T)/\partial(1/T) = U$).

The expression for the internal energy, U , is given by

$$U = \left(\frac{\partial(A/T)}{\partial(1/T)} \right)_{N,v} = \left(\frac{Nqz}{2} \right) \left(\frac{\varepsilon \xi \exp[-\varepsilon/k_B T]}{\xi \exp[-\varepsilon/k_B T] + \xi_h} \right) \quad [A1]$$

and the corresponding integrated result for the Helmholtz free energy, A , is

$$\begin{aligned} \frac{A}{k_B T} = & N \ln \phi + N_h \ln \phi_h + \left(\frac{Nqz}{2} \right) \ln \left(\frac{\xi_h}{\phi} \right) + \left(\frac{N_h z}{2} \right) \ln \left(\frac{\xi_h}{\phi_h} \right) \\ & - \left(\frac{Nqz}{2} \right) \ln \left[\xi \exp[-\varepsilon/k_B T] + \xi_h \right] \end{aligned} \quad [A2]$$

with definitions:

$$\begin{aligned} N_h &= (V/v) - Nr; & \phi &= Nrv/V; & \phi_h &= N_h v/V; \\ qz &= rz - 2r + 2; & \xi &= Nq/(Nq + N_h); & \xi_h &= N_h/(Nq + N_h) \end{aligned}$$

In the definitions, N_h is the number of *vacant* lattice sites ("h" stands for "holes") and V/v is the *total* number of lattice sites. ϕ is the volume fraction of segments, and ϕ_h is the volume fraction of vacant sites. z is the lattice coordination number which is fixed at a value of $z = 6$. (Using other fixed values of z (e.g., $z = 8$ or 10) will cause the optimal values of the parameters r, v, ε to change, but it will not appreciably change the overall quality of the fitted properties.) qz is the total number of possible non-bonded contacts available to a single chain molecule, which follows by subtracting the $(2r-2)$ bonded contacts. ξ and ξ_h are thus "concentration variables" which express fractions of non-bonded contacts, for segments and vacancies respectively, out of the total number of possible non-bonded contacts.

Note that *all* of the free volume in the LCL model ($V_{\text{free}} = V - Nrv = N_h v$) comes from the empty lattice sites (what we call the "holes"); the lattice sites themselves are not compressible. Though this is obviously a coarse-grained picture, the LCL model fits the *PVT* data well (e.g. Figure 4); here the underlying N_h and ϕ_h , etc. are smooth functions that, upon fitting, account in an averaged way for all the varied sized gaps/portions of free volume in a real system. Note that although LCL is a lattice-based model, and though segments don't "explicitly" have vibrations at the lattice sites, all externally coupled vibrational contributions (e.g. those that would cause a solid to expand) must be accounted for, and so, the discretization of the model space adjusts to cover both excess, and the (externally coupled) solid-like vibrational contributions (if one chooses to imagine them divided up this way).

Given the Helmholtz free energy (A) as a function of N, V, T , all of the other thermodynamic properties can be derived using standard thermodynamic relationships. The pressure, P , is

$$P = -\left(\frac{\partial A}{\partial V}\right)_{N,T} = \left(\frac{k_B T}{v}\right) \ln\left(\frac{1}{\phi_h}\right) + \left(\frac{k_B T z}{2v}\right) \ln\left(\frac{\phi_h}{\xi_h}\right) - \left(\frac{k_B T z \xi}{2v}\right) \left(\frac{\xi (\exp[-\varepsilon/k_B T] - 1)}{\xi \exp[-\varepsilon/k_B T] + \xi_h} \right) \quad [\text{A3}]$$

Note this is the same as eq 13 in the main text where in that case for simplicity, the value of fixed $z = 6$ and the other definitions (ϕ , ϕ_h , N_h , etc.) are substituted in. The entropy, S , is also readily obtained from A and U above, that is,

$$S = - \left(\frac{\partial A}{\partial T} \right)_{N,V} = \frac{U}{T} - \frac{A}{T} \quad [A4]$$

As noted in the main text, in order to compare the polymer properties, each polymer must first be characterized within the LCL model. We do this by fitting the expression for the pressure, P , to obtain the characteristic molecular parameters (r, v, ε) that give best agreement for each polymer with its respective pressure-volume-temperature (PVT) data. We fit only to the polymer's equilibrium melt state, and correspondingly, all of the ensuing model property calculations and predictions are thus for the melt only. (The one exception to this was for the case of PS (Figure 4), where we did two characterizations leading to two different parameter sets: one for the melt, and the other for the glass [see further comments below].) The fits typically cover a temperature range of about 80 degrees K centered if possible around $T = 425$ K, and a pressure range that is typically $P = 0$ to 100 MPa (depending at times on data availability). To make the most reliable property comparisons we have found that it is important to make an effort to fit each polymer over as close to the same temperature data range as possible. We have chosen to target (when possible) $T \approx 425$ K for a data range mid-point temperature because it corresponds to a temperature where the most polymer melt data is available. (There are exceptions of course, and further, in a few cases the polymer might be glassy at that T and so we are forced to fit at higher T).

A summary of the characterization results for 51 polymer melts is presented in Appendix Table 1. (Information for the one glassy characterization is in the table footnote.) The table gives the molecular parameters r , v , and ε . For convenience the table also includes the full polymer names and corresponding acronyms, and references to the experimental PVT data (to which the polymers were parameterized), and the experimental T_g values (to which we have compared with

the model properties). We note that the model parameters do correspond to very typical molecular level quantities. For example, a typical value for the segmental volume, v , is 8 mL/mol, which corresponds to 13.3 cubic Angstroms and a segmental length of 2.37 Angstroms. rv , the hard-core molecular volume, a quantity relied on throughout this paper, is always on the order of, but somewhat less than, the total volume per molecule in a liquid, as expected. The nonbonded energetic parameter, ε , is on the order of a typical nonbonded intermolecular interaction energy. The table shows ε values that range around -1500 to -2500 J/mol, which are on the same scale as typical Lennard-Jones parameters, e.g. $\varepsilon_{\text{LJ}} = 996$ J/mol for argon, 1230 J/mol for methane, etc. It can further be verified for small molecules that the cohesive energy per molecule at close packing, $(1/2)(4r+2)\varepsilon$, will be close to the corresponding experimental heat of vaporization. Furthermore, *PVT*-fitted parameters are transferable for predicting mixture properties, and in the case of small molecules, for predicting liquid-vapor equilibria (see examples in refs 44 and 47).

Appendix Table 1. Polymer Characterization Results - Molecular Parameters^a

Acronym	Full Name	T_g (K)	r/M_w (mol/kg)	v (mL/mol)	$-\varepsilon$ (J/mol)	Data Refs <i>PVT</i> / T_g
PS	polystyrene	373	115.29	7.5621	2136.4	53 / 60
PCS	poly(4-chloro styrene)	383	96.50	7.6693	2187.1	53 / 61
PMS	poly(alpha-methyl styrene)	441	104.73	8.0947	2362.9	54 / 60
PIB	polyisobutylene	200	113.87	8.9853	2162.5	53 / 61
PE	polyethylene	231	138.25	7.7962	1930.4	53 / 62
PEPalt	poly(ethylene-co-propylene)alternating	220	124.80	8.6405	1964.2	53 / 63
PEPran	poly(ethylene-co-propylene) random	205	128.42	8.3772	1924.3	53 / 64
aPP	atactic polypropylene	266	118.49	9.0639	1924.2	53 / 65
hhPP	head-to-head polypropylene	245	117.54	8.9583	1965.8	55 / 66
PB-8	polybutadiene (8% 1-2 addition)	179	135.48	7.5407	1930.7	56 / 56
PB-24	polybutadiene (24% 1-2 addition)	188	131.55	7.7844	1933.4	56 / 56
PB-40	polybutadiene (40% 1-2 addition)	203	123.11	8.3173	1956.7	56 / 56
PB-50	polybutadiene (50% 1-2 addition)	212	120.12	8.5018	1953.0	56 / 56
PB-87	polybutadiene (87% 1-2 addition)	259	105.19	9.8423	1985.7	56 / 56
PI-8	polyisoprene (8% 3-4 addition)	210	112.31	9.1620	1993.2	56 / 56
PI-14	polyisoprene (14% 3-4 addition)	214	121.80	8.3671	1981.4	56 / 56
PI-41	polyisoprene (541% 3-4 addition)	236	121.41	8.3888	1976.9	56 / 56
PI-56	polyisoprene (56% 3-4 addition)	253	125.42	8.1387	1963.3	56 / 56
natRBR	natural rubber	201	130.37	7.7456	1962.9	53 / 61

PAA	poly(acrylic acid)	394	124.31	5.2061	2478.1	53 / 67
PMA	poly(methyl acrylate)	282	118.86	6.3718	1998.8	53 / 68
PEA	poly(ethyl acrylate)	250	112.11	7.2549	1893.7	53 / 68
PPA	poly(n-propyl acrylate)	236	109.24	7.8445	1940.4	53 / 68
PBA	poly(n-butyl acrylate)	224	114.99	7.5848	1880.8	53 / 68
PMAA	poly(methacrylic acid)	430	129.71	5.4351	2341.5	53 / 60
PMMA	poly(methyl methacrylate)	378	110.71	6.9576	2177.7	53 / 68
PEMA	poly(ethyl methacrylate)	336	127.82	6.2985	1917.9	53 / 68
PPMA	poly(n-propyl methacrylate)	306	135.17	6.1398	1858.9	53 / 61
PBMA	poly(n-butyl methacrylate)	293	144.02	5.8978	1830.9	53 / 68
PHMA	poly(n-hexyl methacrylate)	268	141.95	6.2656	1803.2	53 / 61
PCHMA	poly(cyclohexyl methacrylate)	377	104.89	7.8733	2129.0	57 / 60
PLMA	poly(lauryl methacrylate)	208	134.61	7.1740	1871.8	53 / 61
PDMS	poly(dimethyl siloxane)	149	84.65	10.9306	1655.2	53 / 69
PEO	poly(ethylene oxide)	232	149.45	5.4156	1899.7	53 / 60
PECH	polyepichlorohydrin	251	90.54	7.4799	2082.8	30 / 60
PC	polycarbonate	420	118.09	6.3724	2104.6	53 / 61
TMPC	tetramethyl bisphenolA polycarbonate	469	88.54	9.3484	2286.0	58 / 58
PPO	poly(phenylene oxide)	480	103.42	7.9638	2166.1	53 / 61
PES	poly(ether sulfone)	490	99.24	6.7126	2588.7	53 / 53
PEI	poly(ethylene isophthalate)	328	134.04	5.0862	2109.5	53 / 70
BphAI	bisphenol A isophthalate	453	103.13	7.2862	2377.3	53 / 71
PNB	polynorbornene	405	113.33	7.9605	2223.5	53 / 53
PVFL	poly(vinyl formal)	335	131.69	5.6890	2037.6	53 / 53
PVBL	poly(vinyl butyral)	325	132.88	6.2508	1918.3	53 / 53
PVF	poly(vinyl fluoride)	337	105.38	6.6886	2150.8	53 / 60
PVDF	poly(vinylidene fluoride)	238	89.66	6.1887	2005.2	53 / 60
PVC	poly(vinyl chloride)	357	126.99	5.1078	2022.3	53 / 61
PVME	poly(vinyl methyl ether)	242	111.53	7.9296	1946.4	59 / 60
PVAc	poly(vinyl acetate)	305	122.88	6.2787	1922.9	53 / 61
PCLA	polycaprolactone	211	126.96	6.6593	1983.7	53 / 72
SAN	poly(styrene-co-acrylonitrile)	380	122.87	6.9214	2164.0	53 / 60

^a The table contains the results from pure component polymer characterization via fitting to *PVT* data. The resulting molecular parameters are: r , the number of segments per chain molecule, v , the volume per lattice site, and ε , the segment-segment nonbonded interaction energy. r is tabulated as r/M_w where M_w is the polymer molecular weight. Also included are references for the experimental T_g and *PVT* data. All values in the table correspond to the polymer melt. Note that one additional characterization was performed on PS glass which gave: $r/M_w = 67.35$ mol/kg, $v = 13.5612$, $\varepsilon = -2951.8$ J/mol.

As a few final comments, we note some details on the distinction between equilibrium melt *PVT* data and glassy data, and the way it is described by Zoller and Walsh (ref 53). Paraphrasing from page 9 in their introduction, they describe the glass as being in a quasi-equilibrium state, which should not change (except over long periods of time or if near the glass transition temperature). The glassy data show all the basic features of liquid data except that the thermal expansivity and isothermal compressibility are all smaller and less dependent on temperature.

An important point with regard to our analysis of the Zoller and Walsh glassy data is how they do their "standard *PVT* run". They take measurements along isotherms (point-wise isothermal compression) starting with the lowest temperature isotherm. (So they start with a glassy sample.) They then raise the temperature (i.e. working from below) for the next run; this way they do not melt or reform the glass until reaching $T =$ the ambient pressure T_g . All data we analyze are at T 's below the ambient pressure T_g , and correspond to a single quasi-equilibrium sample. Other data collection approaches, e.g. cooling from the melt along an isobar at elevated pressure could produce a different, densified glass, but the Zoller and Walsh standard *PVT* run avoids this situation. Our fit to the Zoller and Walsh glassy data draws its basis from the above described "quasi-equilibrium" point of view, and the quality of the fit is evidenced in figure 3. Of course, the properties still depend somewhat on how that *particular* sample glass was formed, and furthermore, of course, the *model* glass cannot age.

Appendix B: Analysis of a *P*-Dependent Free Volume Model

There have been attempts to model the general T, P -dependence of dynamics while maintaining solely a free volume-based point of view. One popular free volume model (described in the book by Ferry, ref 85) has been associated with some misconceptions and unanswered physical questions and so here we offer what we hope will be clarifying comments.

As noted, experiments have made it clear that dynamics still change when V is fixed, that is, they change with P and T as one travels along an isochore. If V comprises a constant hardcore volume plus a total free volume then along an isochore the total free volume must be constant. This means that in order to insist that the (T, P) dependence of dynamic data can be explained by free volume, alone, you cannot link the dynamics to total free volume. In order to persist with a picture whereby dynamics and free volume are correlated one could propose that *excess* free volume is what controls the dynamics, alone, as it could change when V and the

total V_{free} are fixed. The model in ref 85 thus introduced a (phenomenological) T and P dependent functional form for *excess* free volume that depends on two parameters α_{exs} and κ_{exs} (these are inspected below). The dynamic data can be fit to that functional form (within a Doolittle-type equation) and the resulting α_{exs} and κ_{exs} values are interpreted as characterizing how the excess free volume depends on P and T . Now, of course, traveling along an isochore you will get a nonzero change in this "excess" free volume (since the α_{exs} and κ_{exs} values just determined are not the experimental/volumetrically determined melt values), and in order to rationalize this, you have to say that the change in the "occupied volume" (which would be the vibrational piece, in our language) must compensate so that the overall change is zero. This rationalization, though, leads to the unsupported conclusion that (for example) the compressibility (κ_{exs}) of the excess free volume is significantly smaller than the compressibility of the occupied volume. In fact, however, liquids are typically twice as compressible as solids, which implies that contributions from the T -dependence of the excess and the T -dependence of the vibrational (in the "occupied") free volume play comparable roles. The way out of this conundrum is to **not** insist that free volume alone is responsible for changes in dynamic response with T and P . Below is a more technical analysis of what we have just described, for those interested in the details.

The free volume model in ref 85 considered the T and P dependence of *excess* free volume, expressed as

$$(V_{\text{free:exs}}/V) - (V_{\text{free:exs}}/V)_{\text{ref}} = \alpha_{\text{exs}}\Delta T - \kappa_{\text{exs}}\Delta P \\ = (\alpha_L - \alpha_{\text{vib}})\Delta T - (\kappa_L - \kappa_{\text{vib}})\Delta P \quad [\text{A5}]$$

where $\alpha_{\text{exs}} = (1/V)(\partial V_{\text{free:exs}}/\partial T)_P$, and $\kappa_{\text{exs}} = (1/V)(\partial V_{\text{free:exs}}/\partial P)_T$ and where $(V_{\text{free:exs}}/V)_{\text{ref}}$ is the fractional $V_{\text{free:exs}}$ at a reference point and $\Delta T = T - T_{\text{ref}}$ and $\Delta P = P - P_{\text{ref}}$. Eq A5 is equivalent to equation 54 on page 323 of ref 85. Note that what is termed "fractional free volume" (denoted by f) in that reference, is what we term here as "fractional *excess* free volume". In connecting with dynamics, the now more generalized form for $1/(V_{\text{free:exs}}/V)$ in eq A5 could be substituted in the Doolittle eqn,

similar to the description above in Section 1.3 in deriving the original WLF equation where $\alpha_{\text{exs}} = 1/(C_1 C_2)$. (As examples, equations 50 and 61 in ref 85 are obtained for isotherms and isochors respectively.) The second form of eq A5 is helpful in analysis, and it follows from the contributions to the total fractional free volume, (V_{free}/V) , where

$$\begin{aligned}\alpha_L \Delta T - \kappa_L \Delta P &= (V_{\text{free}}/V) - (V_{\text{free}}/V)_{\text{ref}} \\ &= (V_{\text{free:exs}}/V) - (V_{\text{free:exs}}/V)_{\text{ref}} + (V_{\text{free:vib}}/V) - (V_{\text{free:vib}}/V)_{\text{ref}} \\ &= \alpha_{\text{exs}} \Delta T - \kappa_{\text{exs}} \Delta P + \alpha_{\text{vib}} \Delta T - \kappa_{\text{vib}} \Delta P\end{aligned}\quad [\text{A6}]$$

with $\alpha_{\text{vib}} = (1/V)(\partial V_{\text{free:vib}}/\partial T)_P$ and $\kappa_{\text{vib}} = (1/V)(\partial V_{\text{free:vib}}/\partial P)_T$, which correspond to the solid-like contribution (contribution from the "occupied volume"), and with the overall coefficients of thermal expansion and compressibility being $\alpha_L = (1/V)(\partial V/\partial T)_P$ (as used above), and $\kappa_L = (1/V)(\partial V/\partial P)_T$.

Now, start with the assumption that $V_{\text{free:exs}}$ *solely* controls dynamics, and consider the "isochronic" condition, where T and P change so as to produce no net change in dynamics (constant τ). This condition would thus be obtained by setting the change in $V_{\text{free:exs}}$ (eq A5) to zero, thus giving $(\partial P/\partial T)\tau = \alpha_{\text{exs}}/\kappa_{\text{exs}} = (\alpha_L - \alpha_{\text{vib}})/(\kappa_L - \kappa_{\text{vib}})$. This should be contrasted to the conditions of fixed V (fixed total V_{free}), where $0 = \alpha_L \Delta T - \kappa_L \Delta P$, and thus, $(\partial P/\partial T)_V = \alpha_L/\kappa_L$. Given how dynamics still change at constant V , it is thus found experimentally that $(\partial P/\partial T)\tau$ is significantly larger than $(\partial P/\partial T)_V$. So this means that, if $V_{\text{free:exs}}$ solely controls dynamics, $\alpha_{\text{exs}}/\kappa_{\text{exs}} [= (\alpha_L - \alpha_{\text{vib}})/(\kappa_L - \kappa_{\text{vib}})]$ would have to be significantly larger than α_L/κ_L . That is, the excess free volume would have to be less compressible relative to its thermal expansion, than is the overall compressibility relative to overall thermal expansion. Put another way, the vibrational free volume (the "occupied volume") must be significantly more compressible than the excess free volume. This implied result is one of the strange physical consequences of the model, as has been noted in the literature.^{1,4}

So, can the experimental observation, $(\partial P/\partial T)_\tau > (\partial P/\partial T)_V$, be explained by excess free volume behavior such that $\alpha_{\text{exs}}/\kappa_{\text{exs}} > \alpha_L/\kappa_L$? A test would be to calculate an independent *volumetric* estimate of $\alpha_{\text{exs}}/\kappa_{\text{exs}} = (\alpha_L - \alpha_{\text{vib}})/(\kappa_L - \kappa_{\text{vib}})$. Here we choose as an example the glass-forming liquid ortho-terphenyl (OTP) and we take the solid-like vibrational contributions, α_{vib} and κ_{vib} , to be those of its corresponding crystalline solid, along with α_L and κ_L for the liquid; these data are available in Naoke and Koeda.⁸⁹ The values are taken from ref 89 figures 2 and 5 at a temperature a little below the melting temperature ($\alpha_L = 0.0007314 \text{ K}^{-1}$, $\alpha_{\text{vib}} = 0.0002625 \text{ K}^{-1}$, $\kappa_L = 0.00060 \text{ MPa}^{-1}$, $\kappa_{\text{vib}} = 0.00025 \text{ MPa}^{-1}$), and, we obtain from this $\alpha_{\text{exs}}/\kappa_{\text{exs}} = 1.35 \text{ MPa/K}$. Now if, the free volume model in ref 85 is correct, then this $\alpha_{\text{exs}}/\kappa_{\text{exs}}$ value should be close to the dynamically determined $(\partial P/\partial T)_\tau$, and it should not be close to $(\partial P/\partial T)_V$. In fact, experimental $(\partial P/\partial T)_\tau$ values⁹⁰ for OTP are found to typically average around 3.7 MPa/K, much larger than the volumetrically determined $\alpha_{\text{exs}}/\kappa_{\text{exs}}$ (= 1.35 MPa/K). The condition of constant excess free volume *does not* correspond to the condition of constant relaxation time. $\alpha_{\text{exs}}/\kappa_{\text{exs}}$ is in fact, much closer to the value of $(\partial P/\partial T)_V = \alpha_L/\kappa_L = 1.22 \text{ MPa/K}$, and this means that the excess free volume doesn't behave that much differently from the total free volume (conditions when one is fixed are close to when the other is fixed), and an equivalent consequence of this is that, the vibrational free volume (the occupied volume) is not much more compressible than the excess free volume.

Results are similar for polymers: The values for the polymers in Table 11-III in ref 85 have $(\partial P/\partial T)_\tau$ values ranging from 4 to 6 MPa/K, while we expect $\alpha_{\text{exs}}/\kappa_{\text{exs}}$ values to typically be closer to 1 MPa/K. For example, for the PS sample analyzed here, using the glass values to estimate α_{vib} and κ_{vib} , we have $\alpha_L = 0.000619 \text{ K}^{-1}$, $\alpha_G = \alpha_{\text{vib}} = 0.000262 \text{ K}^{-1}$, $\kappa_L = 0.000722 \text{ MPa}^{-1}$, $\kappa_G = \kappa_{\text{vib}} = 0.000412 \text{ MPa}^{-1}$, and we get $\alpha_{\text{exs}}/\kappa_{\text{exs}} = 1.15 \text{ MPa/K}$. This is similar to $\alpha_L/\kappa_L = 0.86 \text{ MPa/K}$, and much different from $(\partial P/\partial T)_\tau \approx 3 \text{ MPa/K}$ (estimated using dT_g/dP in ref 1). It was recognized in ref

85 (pages 323-325), that experimental $(\partial P/\partial T)_\tau$ values would imply that the compressibility of the excess free volume, $\kappa_{\text{exs}} = (\kappa_L - \kappa_{\text{vib}})$ (in terms of the notation here), would have to be small, and to check this, that $(\kappa_L - \kappa_{\text{vib}}) = (\kappa_L - \kappa_G)$ could be considered as an estimate. Our value for PS of $\kappa_G = 0.000412 \text{ MPa}^{-1}$ (a typical value for glassy samples) is not nearly large enough to result in a value for $(\kappa_L - \kappa_G)$ sufficiently small so as to make $\alpha_{\text{exs}}/\kappa_{\text{exs}}$ comparable to $(\partial P/\partial T)_\tau$. It was noted in ref 85, that (paraphrasing) that assuming $\kappa_G = \kappa_{\text{vib}}$ should be done with caution because of the failure of voluminal equilibrium in the glassy state. Evidence for this was depicted in ref 85, FIG. 11-10, a volume-temperature diagram which showed how a particular path of glass formation (pressurizing the melt and then cooling) would lead to the possibility of defining a κ_G that would be larger than if one chose to define κ_G by an isothermal compression. As noted above in describing the Zoller and Walsh standard *PVT* runs, the latter case conforms to the collection of a quasi-equilibrium data set. The former case (leading to the large κ_G favored in ref 85) corresponds to a pressurized glass wherein the *PVT* data (including data at different *P*'s) would not correspond to a single quasi-equilibrium sample. Further, the implication is that significant free space is lost from the vibrational volume by effectively shifting a baseline. In fact, it is actually lost by compressing excess free volume out of the glass. The former case, where κ_G comes from a quasi-equilibrium sample, should be considered the most correct, and thus $\alpha_{\text{exs}}/\kappa_{\text{exs}}$ is too small compared to $(\partial P/\partial T)_\tau$. The points above have admittedly involved a number of assumptions and approximations, so that is why it has been helpful to have available the case using crystalline data for OTP.

Table of Contents Graphic

Polymer Free Volume and Its Connection to the Glass Transition

Ronald P. White and Jane E.G. Lipson

Predictions for Free Volume and Connecting it to Glassy Behavior

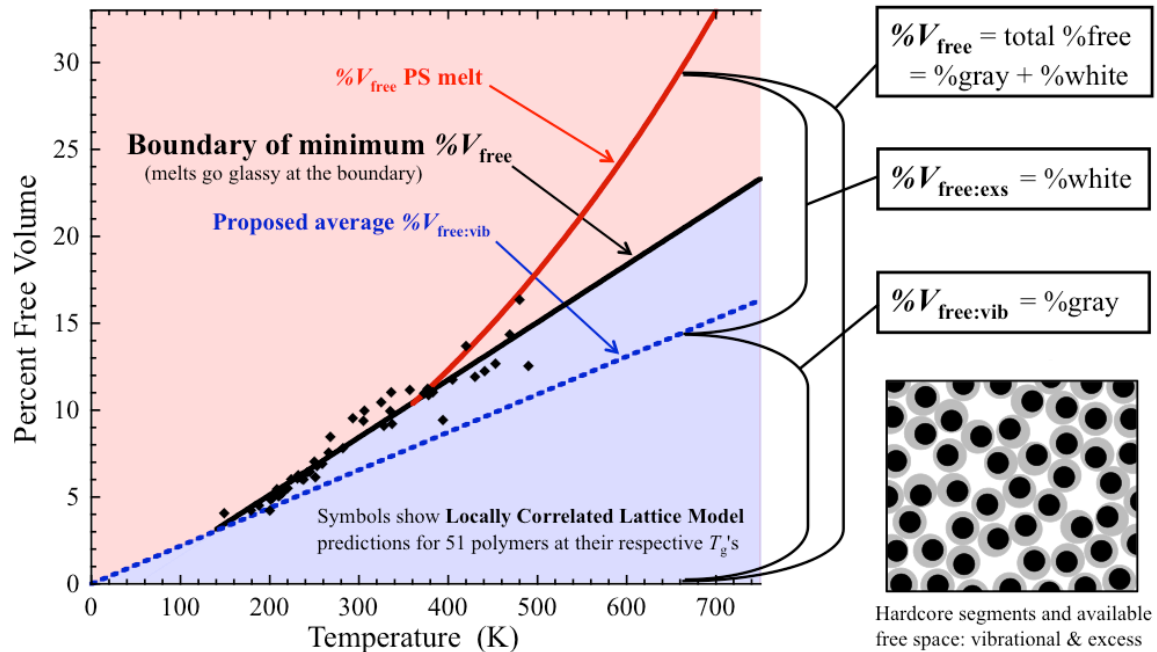


Photo: Ron White



Biography: Ron White

Ron did his graduate studies at the University of New Hampshire (PhD, 2002) and since then has been a post doc/research associate at the University of Pittsburgh and currently, Dartmouth College. Research in grad school included optimization algorithms, statistical mechanics of rare gas clusters, and dynamical modeling applied to mass spectrometry. At Pittsburgh, work focused on molecular simulation methods for evaluating entropic properties, and some simulation work on biomolecules. At Dartmouth, research has covered integral equation theories for lattice-based and continuum chain molecule fluids, developing predictive equations of state for bulk systems and films, and simulation work. Applications have involved polymers, small molecules, and their mixtures; a current focus is on glass-forming systems.

Photo: Jane Lipson



Biography: Jane Lipson

Jane E.G. Lipson earned all her degrees (B.Sc., M.Sc., and Ph.D.) from the University of Toronto. She then shifted to Dartmouth College, working as a NATO Scholar with Walter Stockmayer. After an initial academic appointment at the University of Guelph, she moved back to Dartmouth, rising through the academic ranks in the Chemistry Department where she now holds the Albert W. Smith Chair in Chemistry. She has been a recipient of the Camille and Henry Dreyfus Teacher-Scholar Award, and The Arthur K. Doolittle Award (American Chemical Society), and is a Fellow of the American Physical Society (APS). She has been Chair both of the APS Polymer Physics Division and of the Polymer Physics Gordon Conference. Since 2008 she has served as an Associate Editor for *Macromolecules*. Her research group is focused on deriving and applying theoretical and computational methods to tackle problems involving both miscibility and glassiness in complex fluids, with a particular interest in polymers. A long-standing feature of her research has been an emphasis on holding theory accountable to experiment.